

PREPARED FOR SUBMISSION TO JHEP

Entanglement Temperature in Non-conformal Cases

Song He,^a Danning Li,^b Jun-Bao Wu^b

^a*State Key Laboratory of Theoretical Physics, Institute of Theoretical Physics, Chinese Academy of Science, Beijing 100190, P. R. China*

^b*Institute of High Energy Physics, and Theoretical Physics Center for Science Facilities, Chinese Academy of Sciences, Beijing 100049, P.R. China*

E-mail: hesong@itp.ac.cn, lidn@ihep.ac.cn, wujb@ihep.ac.cn

ABSTRACT: Potential reconstruction can be used to find various analytical asymptotical AdS solutions in Einstein dilation system generally. We have generated two simple solutions without physical singularity called zero temperature solutions. We also proposed a numerical way to obtain black hole solution in Einstein dilaton system with special dilaton potential. By using this method, we obtain the corresponding black hole solutions numerically and investigate the thermal stability of the black hole by comparing the free energy of thermal gas and the corresponding black hole. In two groups of non-conformal gravity solutions obtained in this paper, we find that the two thermal gas solutions are more unstable than black hole solutions respectively. Finally, we consider black hole solutions as a thermal state of zero temperature solutions to check that the first thermal dynamical law exists in entanglement system from holographic point of view.

KEYWORDS: Black hole solutions, Thermal gas solutions, Entanglement temperature, AdS/CFT correspondence

Contents

1	Introduction	1
2	Einstein-Maxwell-Dilaton system	3
2.1	Potential reconstruction in domain wall ansatz	6
3	General asymptotical AdS black hole solutions	7
3.1	The first analytical solution	8
3.1.1	The corresponding black hole solution	9
3.2	The second analytical solution	11
3.2.1	The corresponding black hole solution	13
4	Energy momentum tensor and free energy	16
4.1	Energy momentum tensor	16
4.2	The difference of free energy	18
5	Entanglement temperature	20
5.1	Variation of entanglement entropy in strip case	20
5.2	Entanglement temperature in strip case	22
6	Conclusion and discussion	26
	Appendices	27
A	Appendix: Search of the Black Hole Solution Numerically	27
A.1	The first numerical black hole solution	29
A.2	The second numerical black hole solution	31
B	Other Analytic Solutions	32

1 Introduction

The AdS/CFT correspondence [1][2][3][4] is a very important and fundamental relation which connects gravitational theories and quantum field theories. As an application, in [5] Ryu and Takayanagi proposed a general way for calculating the entanglement entropy of boundary field theory through AdS/CFT correspondence. The main point is that the entanglement entropy in the large N (and large 't Hooft coupling) limit in field theory side can be mapped to an area of minimal surface in gravity side. Prescription on computing the holographic entanglement entropy (HEE) has been proved in [6][7]. There are so many

evidences [8][9][10] to confirm this proposal within AdS_3/CFT_2 correspondence. As applications of HEE, there are intensive studies [11]–[26] recently. More recently, in [27], a free falling particle in an AdS space was used to mimic the holographic dual of local quenches and the HEE has been computed to show the evolution of quantum entanglement. In [28], an analytical framework for holographic counterpart of global quantum quenches was given. In [29], the authors studied how a small perturbation of HEE evolves dynamically through solving the Einstein equation in AdS spaces.

In vacuum state the leading divergent term of entanglement entropy (EE) is proportional to the area of the entangling surface (in many models)[30][31], which is the original motivation for relating EE with black hole entropy. The EE is also an useful quantity to describe the quantum correlations between the in and out side of a subsystem in QFT. The behavior of EE in low excited states is also important to understand the quantum entanglement nature of the system. This topic has been studied by many authors, for example [32][33]. The elegant method of HEE could also be used to study the property of EE in low excited states of CFT, which may be related with the background perturbation of the bulk.

In [35], the authors have studied the low thermal excited state in the holographic view, and furthermore, they find an interesting relation between the variance of energy and EE of the subsystem in low thermal excited states of CFT living on the boundary, which is similar to the first law of thermodynamics, i.e., $\Delta E = T_{eff} \Delta S$, where T_{eff} , called entanglement temperature, is only related to the shape of the subsystem.

In effective theory of gravity, higher derivative terms will appear as corrections to Einstein-Hilbert action. The HEE formula for Lovelock gravity have been studied in [15][16] by comparing the logarithm term with the CFT prediction¹. [23][36] have also studied the HEE with higher derivative gravity. In [37], the authors have studied the property of EE with low excitation in these cases from the the holographical point of view. Though general formula of HEE with the bulk theory containing arbitrary higher curvature terms is still an open question to be further studied, one can still hope that the results in [15][16][17][18][23][36][38][37] will shed light on the quantum corrections to HEE. More recently, some quantum corrections have been studied in [39][40].

We would like to extend these studies to non-conformal cases, especially for Einstein-dilaton system. The key point of this extension is to find vacuum state and corresponding thermal excitation state. Previously, there were various studies in [41] [42] on gravity solutions in ED system. It is hard to obtain the gravity duals of these two states in these frameworks. Different from the logic of [41] [42], a bottom-up approach known as the potential reconstruction approach [43][44] is indeed a much easier way to obtain gravity solutions. Using this bottom-up approach, a new Schwarzschild-AdS black hole in five-dimensions coupled to a scalar field was discussed in [43], while dilatonic black hole solutions with a Gauss-Bonnet term in various dimensions were discussed in [45]. A new class of four dimensional gravity solutions has been found in [46].

We will review the potential reconstruction approach to obtain general gravity so-

¹HEE in this case was also studied in [17][18], following the approach of [6].

lution in 5D. In [44], the authors have used this method to construct a semianalytical gravity solution to study some thermodynamical quantities, their results agree with the numerical results from recent studies in lattice QCD. [44] provided an excellent example of constructing a holographic model using the potential reconstruction approach. Motivated from finding the vacuum state and thermal excitation state, we would like to construct two gravity solutions or phases in the same ED system. It is valuable to study the thermal excitation properties of this system. In this paper, we will list two analytical zero temperature solutions to show the details of this approach.

In this paper, we would like try to obtain two black hole solutions which correspond to these two zero temperature solutions, respectively. To find the gravity solutions in Einstein dilation system with special dilation potential is the hard core. We here propose a systematical way to obtain the numerical gravity solutions. To give the details, we take two black hole solutions obtained in this paper as examples. Furthermore, we have studied the free energy of these solutions and find that the thermal gas solutions are thermal dynamically unstable. By following the logic line proposed by [35], we consider black hole solution as the thermal excitation of corresponding zero temperature solution and we would like study a novel quantity called entanglement temperature. With this entanglement temperature, there exists the first-law-like relation that are proposed in [35] then.

The organization of the paper is as follows: in section 2, we briefly review the potential reconstruction approach to the Einstein-Maxwell-Dilaton system by generalizing the discussion in [47] to the case with a coupling between dilaton field and Maxwell field. We also follow this approach to generate domain wall solutions. In section 3, we discuss the generic black hole solution with asymptotical AdS boundary in Einstein dilaton system, and in particular present two new analytic zero temperature solutions which will be used later. In this section, we also proposed a numerical way to obtain the black hole solutions in ED system. We list two groups of gravity solutions. In each group, the one is zero temperature solution and the other is corresponding black hole solution. In section 4, we calculate the difference of free energy of thermal gas and the corresponding black hole solutions generally. Here these thermal gas solutions are obtained from Wick rotation in time direction in zero temperature solutions. We take two groups of thermal gas and Euclidean version of black hole solutions as examples to show that the thermal gas solutions are unstable. In section 5, as an application of these solutions from AdS/CFT point of view, we study the novel quantity called entanglement temperature in these cases and we consistently check that the thermodynamical first law like exists in our cases. Section 6 is devoted to conclusions and discussions. We put some details of the computations in this paper in the Appendix A. In appendix B, we list 6 new gravity solutions generated by potential reconstruction in ED system.

2 Einstein-Maxwell-Dilaton system

In this section, we just review how to use the potential reconstruction approach [44, 47–49] to obtain solutions to a 5D Einstein-Dilaton (ED) system and Einstein-Maxwell-Dilaton

(EMD) system. In [47], the authors have not considered the coupling between gauge field and dilaton field in Einstein frame. Here we take the coupling into consideration to start with a more general version

$$S_{5D} = \frac{1}{16\pi G_5} \int d^5x \sqrt{-g^S} e^{-2\phi} \left(R^S + 4\partial_\mu \phi \partial^\mu \phi - V_S(\phi) - \frac{Z(\phi)}{4g_g^2} e^{\frac{-4\phi}{3}} F_{\mu\nu} F^{\mu\nu} \right), \quad (2.1)$$

where the action (2.1) is written in string frame, $F_{\mu\nu} = \partial_\mu A_\nu - \partial_\nu A_\mu$ is the Maxwell field. In Einstein frame, we can write the action as [49]

$$S_{5D} = \frac{1}{16\pi G_5} \int d^5x \sqrt{-g^E} \left(R - \frac{4}{3} \partial_\mu \phi \partial^\mu \phi - V_E(\phi) - \frac{Z(\phi)}{4g_g^2} F_{\mu\nu} F^{\mu\nu} \right), \quad (2.2)$$

where $V_S = V_E e^{\frac{-4\phi}{3}}$. The metrics in both frames are connected by the scaling transformation

$$g_{\mu\nu}^S = e^{\frac{4\phi}{3}} g_{\mu\nu}^E. \quad (2.3)$$

The Einstein equations from the action (2.2) read

$$E_{\mu\nu} + \frac{1}{2} g_{\mu\nu}^E \left(\frac{4}{3} \partial_\mu \phi \partial^\mu \phi + V_E(\phi) \right) - \frac{4}{3} \partial_\mu \phi \partial_\nu \phi - \frac{Z(\phi)}{2g_g^2} \left(F_{\mu k} F_\nu{}^k - \frac{1}{4} g_{\mu\nu}^E F_{kl} F^{kl} \right) = 0 \quad (2.4)$$

where $E_{\mu\nu} = R_{\mu\nu} - \frac{1}{2} R g_{\mu\nu}$ is Einstein tensor. When we turn off the gauge field, the EDM system will be reduce to ED system given in appendix A. We here consider the ansatz $A = A_0(z)dt$, $\phi = \phi(z)$ for matter fields and

$$ds_S^2 = \frac{L^2 e^{2A_s}}{z^2} \left(-f(z)dt^2 + \frac{dz^2}{f(z)} + dx^i dx^i \right), \quad (2.5)$$

for the metric in string frame, where L is the radius of AdS_5 space and A_s is the warped factor, a function of coordinate z . In Einstein frame the metric reads

$$\begin{aligned} ds_E^2 &= \frac{L^2 e^{2A_e}}{z^2} \left(-f(z)dt^2 + \frac{dz^2}{f(z)} + dx^i dx^i \right), \\ &= \frac{L^2 e^{2A_s - \frac{4\phi}{3}}}{z^2} \left(-f(z)dt^2 + \frac{dz^2}{f(z)} + dx^i dx^i \right), \end{aligned} \quad (2.6)$$

with $A_e = A_s - 2\phi/3$.

In the metric (2.6), the (t, t) , (z, z) and (x_1, x_1) components of Einstein equations are respectively

$$\begin{aligned} b''(z) + \frac{b'(z)f'(z)}{2f(z)} - \frac{b'(z)^2}{2b(z)} + \frac{4}{9}b(z)\phi'(z)^2 + \frac{A_0'(z)^2 Z(\phi)}{6g_g^2 f(z)} + \frac{V_E(\phi)b(z)^2}{3f(z)} &= 0, \\ \phi'(z)^2 - \frac{9b'(z)f'(z)}{8b(z)f(z)} - \frac{9b'(z)^2}{4b(z)^2} - \frac{3A_0'(z)^2 Z(\phi)}{8g_g^2 b(z)f(z)} - \frac{3V_E(\phi)b(z)}{4f(z)} &= 0, \\ f''(z) + \frac{3b'(z)f'(z)}{b(z)} + \frac{4}{3}f(z)\phi'(z)^2 + \frac{3f(z)b''(z)}{b(z)} - \frac{3f(z)b'(z)^2}{2b(z)^2} - \frac{A_0'(z)^2 Z(\phi)}{2g_g^2 b(z)} + V_E(\phi)b(z) &= 0, \end{aligned} \quad (2.7)$$

where $b(z) = \frac{L^2 e^{2A_e}}{z^2}$, and $A_0(z)$ is electrical potential of Maxwell field. From those three equations one can obtain following two equations which do not contain the dilaton potential $V_E(\phi)$,

$$A_s''(z) + A_s'(z) \left(\frac{4\phi'(z)}{3} + \frac{2}{z} \right) - A_s'(z)^2 - \frac{2\phi''(z)}{3} - \frac{4\phi'(z)}{3z} = 0, \quad (2.8)$$

$$f''(z) + f'(z) \left(3A_s'(z) - 2\phi'(z) - \frac{3}{z} \right) - \frac{z^2 Z(\phi) e^{\frac{4\phi(z)}{3} - 2A_s(z)} A_0'(z)^2}{g_g^2 L^2} = 0. \quad (2.9)$$

Eq.(2.8) is the starting point to find exact solutions of the system. Note that Eq.(2.8) in the EMD system is the same as the one in the Einstein-dilaton system considered in [44][48] and the last term in Eq.(2.9) is an additional contribution related to electrical field. In addition, the EOM of the dilaton field is given as following

$$\frac{8}{3} \partial_z \left(\frac{L^3 e^{3A_s(z) - 2\phi} f(z)}{z^3} \partial_z \phi \right) - \frac{L^5 e^{5A_s(z) - \frac{10}{3}\phi}}{z^5} \partial_\phi V_E(\phi) + \frac{Z'(\phi) b(z) A_0'(z)^2}{2g_g^2} = 0. \quad (2.10)$$

The EOM of the Maxwell field is given as

$$\frac{1}{\sqrt{-g^E}} \partial_\mu \left(\sqrt{-g^E} Z(\phi) F^{\mu\nu} \right) = 0. \quad (2.11)$$

From equations of motion, we can obtain a general solution to the system with given $A_s(z)$, which takes the following form

$$\phi(z) = \int_0^z \frac{e^{2A_s(x)} \left(\frac{3}{2} \int_0^x y^2 e^{-2A_s(y)} A_s'(y)^2 dy + \phi_1 \right)}{x^2} dx + \frac{3A_s(z)}{2} + \phi_0, \quad (2.12)$$

$$A_0(z) = A_{00} + A_{01} \left(\int_0^z \frac{y e^{\frac{2\phi(y)}{3} - A_s(y)}}{Z(\phi(y))} dy \right), \quad (2.13)$$

$$f(z) = \int_0^z x^3 e^{2\phi(x) - 3A_s(x)} \left(\frac{A_{01}^2 \left(\int_0^x \frac{y e^{\frac{2\phi(y)}{3} - A_s(y)}}{Z(\phi(y))} dy \right)}{g_g^2 L^2} + f_1 \right) dx + f_0, \quad (2.14)$$

$$\begin{aligned} V_E(z) = & \frac{e^{-2A_s(z) + \frac{4\phi(z)}{3}} z^2 f(z)}{L^2} 2 \left(- \frac{e^{-2A_s(z) + \frac{4\phi(z)}{3}} Z(\phi(z)) z^2 A_0'(z)^2}{4g_g^2 L^2 f(z)} \right. \\ & - \frac{2(3 + 3z^2 A_s'(z)^2 + 4z\phi'(z) + z^2 \phi'(z)^2 - 2z A_s'(z)(3 + 2z\phi'(z)))}{z^2} \\ & \left. - \frac{f'(z)(-3 + 3z A_s'(z) - 2z\phi'(z))}{2zf(z)} \right), \end{aligned} \quad (2.15)$$

where the $\phi_0, A_{00}, A_{01}, f_0, f_1$ are all integration constants and can be determined by suitable UV and IR boundary conditions. Specially for $Z(\phi) = 1$, the general solution reduces to the one given in [47]. Thus we have reviewed a generic formalism [50] to generate exact solutions of the EMD system with a given $A_s(z)$.

2.1 Potential reconstruction in domain wall ansatz

By using of potential reconstruction approach, one can generate gravity solution as he/she wants. In this subsection, we do not repeat the details and just list the results.

Our starting point is the following Einstein-Maxwell-dilaton action in $d + 1$ spacetime dimensions:

$$I = \frac{1}{16\pi G_{d+1}} \int_{\mathcal{M}} d^{d+1}x \sqrt{-g} \left[R - \frac{Z(\phi)}{4} F^2 - \frac{1}{2} (\partial\phi)^2 + V(\phi) \right] + I_{GH}, \quad (2.16)$$

$$I_{GH} = \frac{2}{16\pi G_{d+1}} \int_{\partial\mathcal{M}} d^d x \sqrt{h} K. \quad (2.17)$$

This action describes the dynamics of a $U(1)$ gauge field \mathbf{A}_μ (with field strength $F = d\mathbf{A}$) and a real scalar field ϕ coupled to Einstein gravity. The boundary term I_{GH} is the standard Gibbons-Hawking term needed to make the variational problem well-defined. As such this action describes the grand canonical ensemble.

Since we are interested in solutions with finite temperature and chemical potential and we set following domain wall ansatz

$$ds^2 = e^{2A(u)} (-f(u) dt^2 + dx^i dx^i) + \frac{du^2}{f(u)}, \mathbf{A} = A_t(u) dt, \phi = \phi(u), \quad (2.18)$$

where the AdS radius has been set to one. In this frame the second order equations of motion reduce to the following set of differential equations

$$\frac{d}{du} (e^{(d-2)A} Z \dot{A}_t) = 0, \quad (2.19)$$

$$2(d-1)\ddot{A} + \dot{\phi}^2 = 0, \quad (2.20)$$

$$\ddot{f} + d\dot{A}\dot{f} - e^{-2A} Z \dot{A}_t^2 = 0, \quad (2.21)$$

$$(d-1)\dot{A}\dot{f} + (d(d-1)\dot{A}^2 - \frac{1}{2}\dot{\phi}^2)f - V + \frac{1}{2}Z e^{-2A} \dot{A}_t^2 = 0. \quad (2.22)$$

Here the dot stands for derivative with respect to u . We can extend the logic of potential reconstruction to this general case with domain wall ansatz. The general solutions are as follows

$$\begin{aligned} A_t(u) &= \int_1^u \frac{\rho e^{-2(A(x))}}{Z(\phi(x))} dx + A_{t0}, \\ A &= a_1 u + \int_0^u \left(\int_0^y -\frac{1}{6} \phi'(x)^2 dx \right) dy, \\ f(u) &= \int_0^u \left(e^{-4(Ay)} \int_0^y e^{2(Ax)} (A_t(x))^2 (Z(\phi(x))) dx + f_1 e^{-4(Ay)} \right) dy + f_0, \\ V(u) &= (d-1) (A'(u)) (f'(u)) + (f(u)) \left((d-1)d (A'(u))^2 - \frac{1}{2} (\phi'(u))^2 \right) \\ &\quad + \frac{1}{2} e^{-2(A(u))} (A'_t(u))^2 (Z(\phi(u))), \end{aligned} \quad (2.23)$$

where A_{t0}, a_1, f_0, f_1 are integral constants. One can use the $A(u)$ defined in (2.18) to generate the whole gravity solutions in terms of (2.23). As an application, we here list one explicit solution with $d = 4$:

$$\begin{aligned} A(u) &= u + a, \\ \phi(u) &= b, \\ A_t(u) &= -\frac{c}{2}e^{-2u}, \\ f(u) &= 1 + \frac{c^2 e^{-2a-6u}}{12} - \frac{de^{-4u}}{4}. \\ V(u) &= 12. \end{aligned} \tag{2.24}$$

Here a, b, c, d are integral constants which can be determined by boundary conditions. One can set $a = b = c = d = 0$ to reproduce the pure AdS_5 solution. This example is used to show this method is convenient to generate the gravity solution effectively.

3 General asymptotical AdS black hole solutions

In this part, we will review the general asymptotical AdS black hole solutions given in [50]. Since we are only interested in the black hole solutions with asymptotic AdS boundary, [50] impose the boundary condition $f(0) = 1$ at the AdS boundary $z = 0$, and require $\phi(z), f(z), A_0(z)$ to be regular at black hole horizon z_h and AdS boundary $z = 0$. There is an additional condition $A_0(z_h) = 0$, which corresponds to the physical requirement that $A_\mu A^\mu = g^{tt} A_0 A_0$ must be finite at $z = z_h$.

[50] expressed the function $f(z)$ in eq.(2.14) as

$$f(z) = 1 + \frac{A_{01}^2}{2g_s^2 L^2} \frac{\int_0^z g(x) \left(\int_0^{z_h} g(r) dr \int_r^x \frac{g(y)^{\frac{1}{3}} dy}{Z(\phi(y))} \right) dx}{\int_0^{z_h} g(x) dx} - \frac{\int_0^z g(x) dx}{\int_0^{z_h} g(x) dx}, \tag{3.1}$$

where $f_0 = 1$, $f_1 = -\frac{A_{01}^2}{4g_s^2 L^2} \frac{\int_0^{z_h} g(x) \int_0^x \frac{g(y)^{\frac{1}{3}} dy}{Z(\phi(y))} dy + 1}{\int_0^{z_h} g(x) dx}$ and

$$g(x) = x^3 e^{2\phi(x) - 3A_s(x)}. \tag{3.2}$$

One can expand the gauge field near the AdS boundary to relate the two integration constants to chemical potential and charge density

$$A_0(z) \sim A_{00} + A_{01} \frac{e^{\frac{2\phi(y)}{3} - A_s(y)}}{Z(\phi(y))} \left(1 + y \left(\frac{2\phi'(y)}{3} - A'_s(y) \right) \right) \Big|_{y=0} z^2, \tag{3.3}$$

with

$$A_{00} = \mu, \tag{3.4}$$

$$A_{01} = \frac{\mu}{\int_0^{z_h} y \frac{e^{\frac{2\phi}{3} - A_s(y)}}{Z(\phi(y))} dy} = \frac{\mu}{\int_0^{z_h} \frac{g(y)^{\frac{1}{3}}}{Z(\phi(y))} dy}. \tag{3.5}$$

The temperature of the black hole can be determined through the function $f(z)$ in (3.1) as

$$T = \left| \frac{A_{01}^2}{4\pi g_g^2 L^2} \frac{g(z_h) \int_0^{z_h} g(r) dr \int_r^{z_h} \frac{g^{\frac{1}{3}}(y)}{Z(\phi(y))} dy - g(z_h)}{\int_0^{z_h} g(x) dx} \right|. \quad (3.6)$$

Following the standard Bekenstein-Hawking entropy formula, from the geometry given in eq. (2.6), we obtain the black hole entropy density S , which is obtained using the area A_{area} of the horizon

$$S = \frac{A_{area}}{4G_5 V_3} = \frac{L^3}{4G_5} \left(\frac{e^{A_s - \frac{2}{3}\phi}}{z} \right)^3 \Big|_{z_h}, \quad (3.7)$$

where V_3 is the volume of the black hole spatial directions spanned by coordinates x_i in (2.6). For this paper, we do not consider the effects of the $U(1)$ gauge field. In the remain part, we will focus on the ED system. We will propose an algorithm to obtain the black hole solution in ED system numerically. The algorithm is different from the potential construction approach shown in eq. (2.12)-eq. (2.15). Here we just review the previous results and obtain two zero temperature solutions in different ED systems. It is just technical trick to obtain zero temperature solutions. In the following subsection, we will focus on how to obtain the corresponding black hole solution numerically with respect to special zero temperature solutions in ED system.

3.1 The first analytical solution

In this subsection, we list an analytical solution of the Einstein-Maxwell-Dilaton system by using Eq.(2.12-2.15) with $Z(\phi) = 1$. We impose the constrain $f(0) = 1$, and require $\phi(z), f(z)$ to be regular at $z = 0$, and z_h . We give the solution in Einstein frame

$$ds_E^2 = \frac{L^2 e^{2A_{e1}}}{z^2} \left(-f_1(z) dt^2 + \frac{dz^2}{f_1(z)} + dx^i dx^i \right), \quad (3.8)$$

with

$$\begin{aligned} A_{e1}(z) &= \log \left(\frac{z}{z_0 \sinh(\frac{z}{z_0})} \right), \\ f_1(z) &= 1 - \frac{4V_{11}}{3} (3 \sinh(\frac{z}{z_0})^4 + 2 \sinh(\frac{z}{z_0})^6) + \frac{1}{8} V_{12}^2 \sinh \left(\frac{z}{z_0} \right)^4, \\ \phi_1(z) &= \frac{3z}{2z_0}, \\ A_{01}(z) &= \mu_1 - \frac{2g_g L}{z_0} V_{12} \sinh \left(\frac{z}{2z_0} \right)^2, \end{aligned} \quad (3.9)$$

where z_0 is an integration constant and V_{11}, V_{12} are two constants from the dilaton potential

$$V_{E1}(\phi_1) = -\frac{12 + 9 \sinh^2 \left(\frac{2\phi_1}{3} \right) + 16V_{11} \sinh^6 \left(\frac{\phi_1}{3} \right)}{L^2} + \frac{V_{12}^2 \sinh^6 \left(\frac{2\phi_1}{3} \right)}{8L^2}. \quad (3.10)$$

Note that V_{11} can be parameterized by black hole horizon z_h . The two integration constants V_{11} and V_{12} then can be expressed in terms of horizon z_h as

$$\begin{aligned} V_{11} &= \frac{3\cosh^4\left(\frac{z_h}{2z_0}\right)\left(\frac{\mu^2 z_0^2 \sinh^4\left(\frac{z_h}{z_0}\right)\cosh^4\left(\frac{z_h}{2z_0}\right)}{4g_g^2 L^2} + 8\right)}{32\left(2\sinh^2\left(\frac{z_h}{2z_0}\right) + 3\right)}, \\ V_{12} &= \frac{\mu z_0 \cosh^2\left(\frac{z_h}{2z_0}\right)}{2g_g L}. \end{aligned} \quad (3.11)$$

In this solution, we can just only consider the degenerate case with $V_{11} = 0, V_{12} = 0, \mu_1 = 0$. The explicit form for the degenerate case called the first zero temperature solution is

$$\begin{aligned} A_{et1}(z) &= \log\left(\frac{3p_1 z}{2\sinh\left(\frac{3p_1 z}{2}\right)}\right), \\ f_{t1}(z) &= 1, \\ \phi_{t1}(z) &= p_1 z, \\ V_{Et1}(\phi) &= -\frac{12 + 9\sinh^2\left(\frac{2\phi_{t1}}{3}\right)}{L^2}. \end{aligned} \quad (3.12)$$

In the last step we have set $z_0 = \frac{2}{3}p_1$ which is helpful for following analysis.

3.1.1 The corresponding black hole solution

In this subsection, we would like to find the black hole solution with the same potential as the previous subsection in ED system. Firstly, the UV behavior of the black hole should be asymptotical AdS and there is a horizon in the IR region which is parameterized by z_h . We find an algorithm to find the numerical solution consistently. In order to show how the algorithm work, we list all the details in appendix. Roughly speaking, we try to expand in power series all unknown function as positive powers of z and try to fix all the coefficients numerically. In the UV region, the black hole can be solved as follows from

coupled equations of motion with the potential Eq. (3.12)

$$\begin{aligned}
\phi_{b1}(z) &= p_1 z + p_3 z^3 + \frac{((405f_{41}p_1 + 612p_1^2p_3)z^5)}{3240} \\
&+ \frac{(8100f_{41}p_1^3 + 229635f_{41}p_3 + 10944p_1^4p_3 + 133164p_1p_3^2)z^7}{612360} + O(z^7) \\
f_{b1}(z) &= 1 - f_{41}z^4 - \frac{4}{27}f_{41}p_1^2z^6 + \frac{-13f_{41}p_1^4}{1215} - \frac{f_{41}p_1p_3}{5}z^8 \\
&+ \frac{(-10935f_{41}^2p_1^2 - 328f_{41}p_1^6 - 37908f_{41}p_1^3p_3 - 78732f_{41}p_3^2)z^{10}}{688905} + O(z^{10}) \\
A_{eb1}(z) &= -(2/27)p_1^2z^2 + \left(\frac{4p_1^4}{3645} - \frac{(2p_1p_3)}{15}\right)z^4 \\
&+ \frac{(-54675f_{41}p_1^2 - 128p_1^6 - 67068p_1^3p_3 - 393660p_3^2)z^6}{4133430} \\
&+ \frac{((-50625f_{41}p_1^4 + 64p_1^8 - 3444525f_{41}p_1p_3 - 74952p_1^5p_3 - 2943216p_1^2p_3^2)z^8)}{62001450} \\
&+ O(z^8). \tag{3.13}
\end{aligned}$$

One can see the black hole solution in the UV region can be expressed in series of powers of z . In principle, one can obtain more higher powers of z to get the full expression of black hole background. Unfortunately, we can not obtain complete form of the black hole solution. The main reason is that we do not find simple recurrence relation among the coefficients of each power of z . It is easy to see that the black hole solution with asymptotical AdS can be controlled by three integral constants p_1, p_3, f_{41} . p_1 is free parameter and p_3, f_{41} are determined by boundary condition in IR region. Here we choose parameters p_1, p_3, f_{41} to show one black hole solution numerically. Here p_3, f_{41} are not independent and they are related to the horizon position z_h such that $f_{b1}(z_h) = 0$. In appendix A, we will show the details how to find z_h . The numerical relation between $p_3(z_h)$ and $f_{41}(z_h)$ has been shown in Fig. 1.

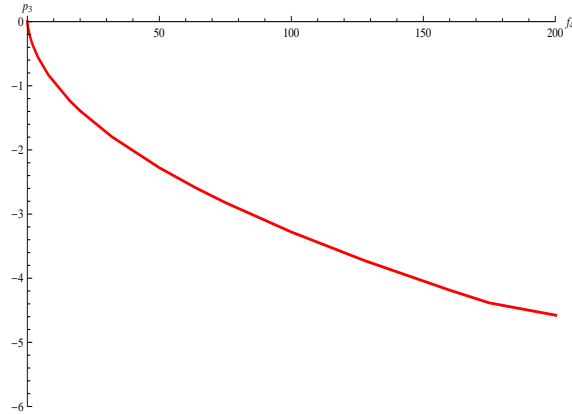


Figure 1. p_3 v.s. f_{41} . p_3 decreasing with f_{41} monotonously. Here we have chosen the parameter $p_1 = 1.5\text{GeV}$.

For simplifying numerical analysis, we fix $p_1 = 1.5\text{GeV}$. Here we just only show the series expansion of black hole solutions and the complete solution can be obtained by the algorithm explained in appendix A. Figs. 2-4 show the configuration of black hole solution. The black hole horizon can be easily read out by $f_{b1}(z_h) = 0$. From these figures, one can continuously go back to zero temperature solution from black hole solution with decreasing value of f_{41} to zero. f_{41} decreases with increasing p_3 simultaneously. Where the temperature is defined by $T = \frac{f_{b1}(z)'}{4\pi}|_{z=z_h}$. This behavior will be helpful to understand entanglement temperature in section 5.

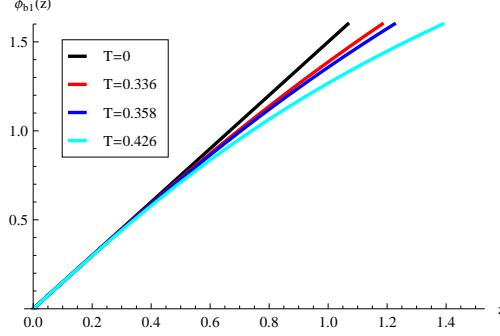


Figure 2. The configuration of $\phi_{b1}(z)$ as a function holographic coordinate z . Here we have fixed $p_1 = 1.5\text{GeV}$ all over the paper. The four parameters for these curves are taken values as following $\{T = 0, f_{41} = 0, p_3 = 0\}$, $\{T = 0.336\text{GeV}, f_{41} = 0.5\text{GeV}^4, p_3 = -0.139...\text{GeV}^3\}$, $\{T = 0.358\text{GeV}, f_{41} = 0.75\text{GeV}^4, p_3 = -0.186...\text{GeV}^3\}$, $\{T = 0.426, f_{41} = 2\text{GeV}^4, p_3 = -0.360...\text{GeV}^3\}$ respectively. To get a smooth function numerically, p_3 have very high-precision and we replace the more additional number with "..." for short.

3.2 The second analytical solution

The second exact solution with ansatz

$$ds_E^2 = \frac{L^2 e^{2A_{e2}}}{z^2} \left(-f_2(z) dt^2 + \frac{dz^2}{f_2(z)} + dx^i dx^i \right), \quad (3.14)$$

is

$$A_{e2}(z) = -\log \left(1 + \frac{z}{z_0} \right), \quad (3.15)$$

$$f_2(z) = 1 - V_{21} \left(\frac{z^7}{7z_0^7} + \frac{z^6}{2z_0^6} + \frac{3z^5}{5z_0^5} + \frac{z^4}{4z_0^4} \right) + \frac{\rho_2^2 z_0^8}{g_g^2 L^2} \left(\frac{5z^8}{32z_0^8} + \frac{z^{10}}{60z_0^{10}} + \frac{z^9}{12z_0^9} + \frac{11z^7}{84z_0^7} + \frac{z^6}{24z_0^6} \right), \quad (3.16)$$

$$\phi_2(z) = 3\sqrt{2} \sinh^{-1} \left(\sqrt{\frac{z}{z_0}} \right),$$

$$A_{02}(z) = \mu_2 + \rho_2 \left(\frac{z_0 z^2}{2} + \frac{z^3}{3} \right). \quad (3.17)$$

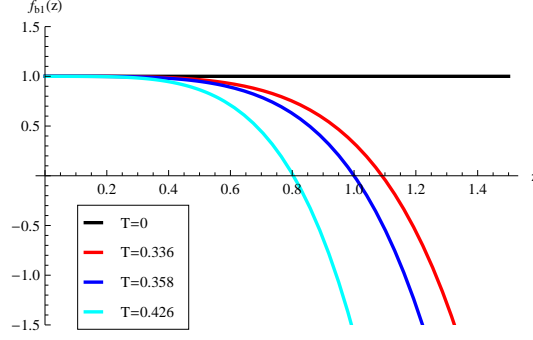


Figure 3. The configuration of $f_{b1}(z)$ as a function holographic coordinate z . Here we have fixed $p_1 = 1.5\text{GeV}$ all over the paper. The four parameters for these curves are taken values as following $\{T = 0, f_{41} = 0, p_3 = 0\}$, $\{T = 0.336\text{GeV}, f_{41} = 0.5\text{GeV}^4, p_3 = -0.139...\text{GeV}^3\}$, $\{T = 0.358\text{GeV}, f_{41} = 0.75\text{GeV}^4, p_3 = -0.186...\text{GeV}^3\}$, $\{T = 0.426, f_{41} = 2\text{GeV}^4, p_3 = -0.360...\text{GeV}^3\}$ respectively. To get a smooth function numerically, p_3 have very high-precision and we replace the more additional number with "..." for short.

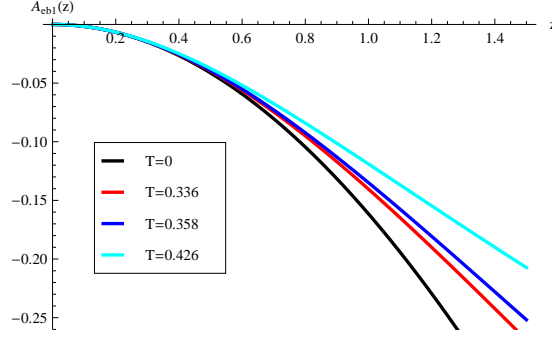


Figure 4. The configuration of $A_{eb1}(z)$ as a function holographic coordinate z . Here we have fixed $p_1 = 1.5\text{GeV}$ all over the paper. The four parameters for these curves are taken values as following $\{T = 0, f_{41} = 0, p_3 = 0\}$, $\{T = 0.336\text{GeV}, f_{41} = 0.5\text{GeV}^4, p_3 = -0.139...\text{GeV}^3\}$, $\{T = 0.358\text{GeV}, f_{41} = 0.75\text{GeV}^4, p_3 = -0.186...\text{GeV}^3\}$, $\{T = 0.426, f_{41} = 2\text{GeV}^4, p_3 = -0.360...\text{GeV}^3\}$ respectively. To get a smooth function numerically, p_3 have very high-precision and we replace the more additional number with "..." for short.

where z_0, μ_2 , and ρ_2 are integration constants and V_{21} is a constant from the dilaton potential and g_g is gauge coupling. The dilaton potential is given as

$$\begin{aligned}
V_{E2}(\phi_2) = & -\frac{12}{L^2} - \frac{42 \sinh^4\left(\frac{\phi_2}{3\sqrt{2}}\right)}{L^2} - \frac{42 \sinh^2\left(\frac{\phi_2}{3\sqrt{2}}\right)}{L^2} \\
& - \frac{3V_{21} \sinh^{14}\left(\frac{\phi_2}{3\sqrt{2}}\right)}{35L^2} - \frac{3V_{21} \sinh^{12}\left(\frac{\phi_2}{3\sqrt{2}}\right)}{10L^2} - \frac{3V_{21} \sinh^{10}\left(\frac{\phi_2}{3\sqrt{2}}\right)}{10L^2} \\
& + \frac{\rho^2 z_0^8}{g_g^2 L^2} \left\{ \frac{\sinh^{24}\left(\frac{\phi_2}{3\sqrt{2}}\right)}{20L^2} + \frac{3 \sinh^{22}\left(\frac{\phi_2}{3\sqrt{2}}\right)}{10L^2} + \frac{59 \sinh^{20}\left(\frac{\phi_2}{3\sqrt{2}}\right)}{80L^2} \right. \\
& \left. + \frac{15 \sinh^{18}\left(\frac{\phi_2}{3\sqrt{2}}\right)}{16L^2} + \frac{5 \sinh^{16}\left(\frac{\phi_2}{3\sqrt{2}}\right)}{-12L^2} + \frac{5 \sinh^{14}\left(\frac{\phi_2}{3\sqrt{2}}\right)}{28L^2} \right\}. \tag{3.18}
\end{aligned}$$

This solution is also a generalization of the one given in [44].

Here we turn off the $U(1)$ gauge field and the second solution can be reduced to the following

$$A_{et2}(z) = -\log\left(1 + p_{\frac{1}{2}}^2 z\right), \quad (3.19)$$

$$f_{t2}(z) = 1, \quad (3.20)$$

$$\phi_{t2}(z) = 3\sqrt{2} \sinh^{-1}\left(p_{\frac{1}{2}}\sqrt{z}\right),$$

$$V_{Et2}(\phi_{t2}) = -\frac{12}{L^2} - \frac{42 \sinh^4\left(\frac{\phi_{t2}}{3\sqrt{2}}\right)}{L^2} - \frac{42 \sinh^2\left(\frac{\phi_{t2}}{3\sqrt{2}}\right)}{L^2}. \quad (3.21)$$

Which is so called the second zero temperature solution. In the last step we have set $z_0 = \frac{1}{\sqrt{p_{\frac{1}{2}}}}$ which is helpful for following analysis.

3.2.1 The corresponding black hole solution

In this subsection, we would like to find the black hole solution with same potential in Einstein dilation system. As before, the UV behavior of the black hole should be asymptotical AdS and there is a horizon in the IR region which is parameterized by z_h . The series expansion of solution near UV region is:

$$\begin{aligned} \phi_{b2}(z) &= p_{\frac{1}{2}}\sqrt{z} - \frac{1}{108}p_{\frac{1}{2}}^3 z^{3/2} + \frac{p_{\frac{1}{2}}^5 z^{5/2}}{4320} + \frac{\left(653184p_{\frac{7}{2}} - 5p_{\frac{1}{2}}^7\right) z^{7/2}}{653184} \\ &+ \frac{z^{9/2} \left(18895680f_{42}p_{\frac{1}{2}} + 515p_{\frac{1}{2}}^9 + \frac{171}{2} \left(653184p_{\frac{7}{2}} - 5p_{\frac{1}{2}}^7\right) p_{\frac{1}{2}}^2\right)}{302330880} \\ &+ \frac{z^{11/2} \left(69284160f_{42}p_{\frac{1}{2}}^3 + 1135p_{\frac{1}{2}}^{11} + \frac{517}{2} \left(653184p_{\frac{7}{2}} - 5p_{\frac{1}{2}}^7\right) p_{\frac{1}{2}}^4\right)}{13302558720} \\ &+ O(z^{\frac{11}{2}}), \\ f_{b2}(z) &= 1 - f_{42}z^4 - \frac{1}{15}2f_{42}p_{\frac{1}{2}}^2 z^5 - \frac{1}{162}f_{42}p_{\frac{1}{2}}^4 z^6 - \frac{f_{42}p_{\frac{1}{2}}^6 z^7}{10206} \\ &+ z^8 \left(-\frac{f_{42}p_{\frac{1}{2}}^8}{1119744} - \frac{f_{42} \left(653184p_{\frac{7}{2}} - 5p_{\frac{1}{2}}^7\right) p_{\frac{1}{2}}}{5598720} \right) \\ &+ \frac{z^9 \left(-35f_{42}p_{\frac{1}{2}}^{10} - 7f_{42} \left(653184p_{\frac{7}{2}} - 5p_{\frac{1}{2}}^7\right) p_{\frac{1}{2}}^3 - 839808f_{42}^2 p_{\frac{1}{2}}^2\right)}{151165440} \\ &+ O(z^{10}), \end{aligned} \quad (3.22)$$

$$\begin{aligned}
A_{eb2}(z) = & -\frac{1}{18}p_{\frac{1}{2}}^2 z + \frac{1}{648}p_{\frac{1}{2}}^4 z^2 - \frac{p_{\frac{1}{2}}^6 z^3}{17496} + \left(\frac{p_{\frac{1}{2}}^8}{559872} - \frac{p_{\frac{1}{2}} \left(653184p_{\frac{7}{2}} - 5p_{\frac{1}{2}}^7 \right)}{8398080} \right) z^4 \\
& + \frac{z^5 \left(-2519424f_{42}p_{\frac{1}{2}}^2 - 109p_{\frac{1}{2}}^{10} - 9 \left(653184p_{\frac{7}{2}} - 5p_{\frac{1}{2}}^7 \right) p_{\frac{1}{2}}^3 \right)}{604661760} \\
& + \frac{z^6 \left(-37791360f_{42}p_{\frac{1}{2}}^4 + 325p_{\frac{1}{2}}^{12} - 159 \left(653184p_{\frac{7}{2}} - 5p_{\frac{1}{2}}^7 \right) p_{\frac{1}{2}}^5 \right)}{228562145280} \\
& + O(z^6).
\end{aligned} \tag{3.23}$$

One can see the black hole solution in the UV region can be expressed in series of powers of z . In principle, one can obtain more higher powers of z to produce the full expression of black hole background. Unfortunately, we can not obtain complete form of the black hole solution. The main reason is still that we also do not find recurrence relation among the coefficients of each power of z . It is easy to see that the black hole solution with asymptotical AdS can be controlled by three integral constants $p_{\frac{1}{2}}, p_{\frac{7}{2}}, f_{42}$. $p_{\frac{1}{2}}$ is free and $p_{\frac{1}{2}}, p_{\frac{7}{2}}, f_{42}$ are determined by boundary condition in IR region. In this case, $p_{\frac{7}{2}}, f_{42}$ are not independent and they are determined by the black hole horizon z_h . The numerical relation between $p_{\frac{7}{2}}$ and f_{42} has been shown in Fig. 5.

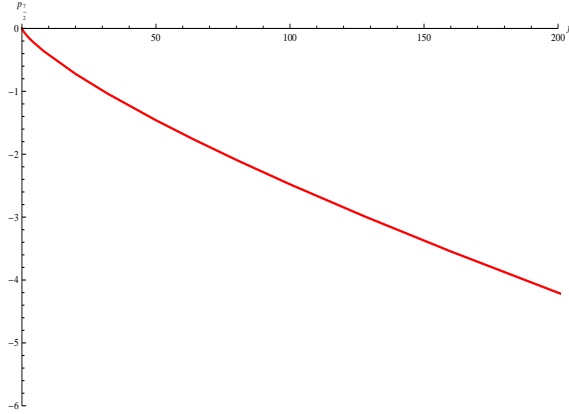


Figure 5. $p_{\frac{7}{2}}$ v.s. f_{42} . $p_{\frac{7}{2}}$ decreasing with f_{42} monotonously. Here we have chosen the parameter $p_{\frac{1}{2}} = 1\text{GeV}$.

For simplifying, we choose groups of $p_{\frac{1}{2}} = 1\text{GeV}^{\frac{1}{2}}$ in this paper. Here we fix parameters $p_{\frac{7}{2}}, f_{42}$ to show black hole solutions numerically in Fig. 6-8. Finally, one can obtain the zero temperature solution with setting $p_{\frac{1}{2}} = 1\text{GeV}^{\frac{1}{2}}, p_{\frac{7}{2}} = 0, f_{42} = 0$. Tuning on $p_{\frac{7}{2}}, f_{42}$ correspond to thermal excitation of zero temperature solution and one also have seen this phenomenon in the first group of solution. In the next section, we will calculate the difference of free energy between the Euclidean black hole and thermal gas obtained by Euclidean zero temperature solution to prove thermal gas is more unstable than black

hole. In this case, turning on small value of f_{42} correspond the thermal excitation from zero temperature solution. Simultaneously, f_{42} increases from zero to small positive value corresponds that decreasing $p_{\frac{7}{2}}$ from zero to small negative number. That is to say the black hole solution can be degenerated to zero temperature solution continuously with setting $f_{42} = 0, p_{\frac{7}{2}} = 0$. Where the temperature is defined by $T = \frac{f_{b2}(z)'}{4\pi}|_{z=z_h}$. Similar consequence applies for the first group of solutions.

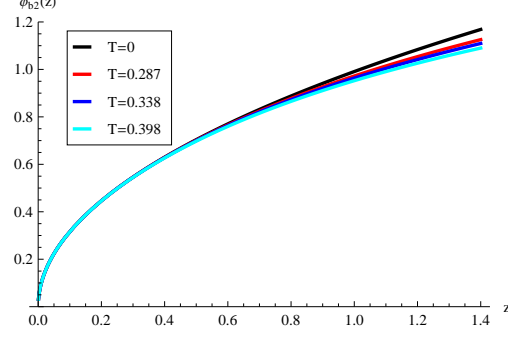


Figure 6. The configuration of $\phi_{b2}(z)$ as a function holographic coordinate z . Here we have fixed $p_{\frac{1}{2}} = 1\text{GeV}^{\frac{1}{2}}$ all over the paper, and the four curves' parameters is as following $\{T = 0, f_{42} = 0, p_{\frac{7}{2}} = 0\}$, $\{T = 0.287\text{GeV}, f_{42} = 0.5\text{GeV}^4, p_{\frac{7}{2}} = -0.040...\text{GeV}^{\frac{7}{2}}\}$, $\{T = 0.338\text{GeV}, f_{42} = 1.0\text{GeV}^4, p_{\frac{7}{2}} = -0.070...\text{GeV}^{\frac{7}{2}}\}$, $\{T = 0.398\text{GeV}, f_{42} = 2.0\text{GeV}^4, p_{\frac{7}{2}} = -0.121...\text{GeV}^{\frac{7}{2}}\}$. To get a smooth function numerically, $p_{\frac{7}{2}}$ have very high-precision and we replace the more additional number with "..." for short.

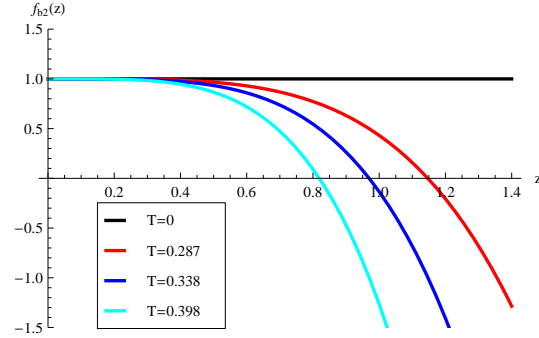


Figure 7. The configuration of $f_{b2}(z)$ as a function holographic coordinate z . Here we have fixed $p_{\frac{1}{2}} = 1\text{GeV}^{\frac{1}{2}}$ all over the paper, and the four curves' parameters is as following $\{T = 0, f_{42} = 0, p_{\frac{7}{2}} = 0\}$, $\{T = 0.287\text{GeV}, f_{42} = 0.5\text{GeV}^4, p_{\frac{7}{2}} = -0.040...\text{GeV}^{\frac{7}{2}}\}$, $\{T = 0.338\text{GeV}, f_{42} = 1.0\text{GeV}^4, p_{\frac{7}{2}} = -0.070...\text{GeV}^{\frac{7}{2}}\}$, $\{T = 0.398\text{GeV}, f_{42} = 2.0\text{GeV}^4, p_{\frac{7}{2}} = -0.121...\text{GeV}^{\frac{7}{2}}\}$. To get a smooth function numerically, $p_{\frac{7}{2}}$ have very high-precision and we replace the more additional number with "..." for short.

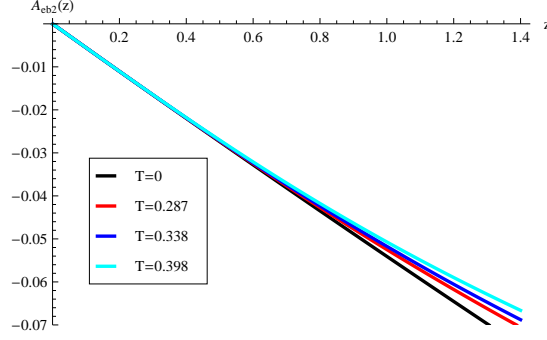


Figure 8. The configuration of $A_{eb2}(z)$ as a function holographic coordinate z . Here we have fixed $p_{\frac{1}{2}} = 1\text{GeV}^{\frac{1}{2}}$ all over the paper, and the four curves' parameters is as following $\{T = 0, f_{42} = 0, p_{\frac{7}{2}} = 0\}$, $\{T = 0.287\text{GeV}, f_{42} = 0.5\text{GeV}^4, p_{\frac{7}{2}} = -0.040...\text{GeV}^{\frac{7}{2}}\}$, $\{T = 0.338\text{GeV}, f_{42} = 1.0\text{GeV}^4, p_{\frac{7}{2}} = -0.070...\text{GeV}^{\frac{7}{2}}\}$, $\{T = 0.398\text{GeV}, f_{42} = 2.0\text{GeV}^4, p_{\frac{7}{2}} = -0.121...\text{GeV}^{\frac{7}{2}}\}$. To get a smooth function numerically, $p_{\frac{7}{2}}$ have very high-precision and we replace the more additional number with "..." for short.

4 Energy momentum tensor and free energy

In this section, we would like to study the stability of thermal gas solutions and Euclidean black hole solutions by comparing the free energy. Here we should stress that thermal gas solution is obtained by Euclidean version of zero temperature solution as mentioned previously [55]. To obtain reasonable energy momentum tensor on the boundary, one should introduce the suitable counter terms. For later use, we just focus on these two groups of thermal gas solutions and black hole solutions. One will see these two groups of solutions capture different characters of UV behaviors. These characters will lead to different behaviors of entanglement temperature which will be studied in the next section.

4.1 Energy momentum tensor

In this subsection, we would like to introduce the counter terms to cancel the divergent of the action and make the energy momentum tensor of dual field theory well defined. In our cases, one can find that we have to introduce ϕ^2, ϕ^4, ϕ^6 terms to cancel the divergences. For ϕ^2 term, it is introduced as standard AdS/CFT dictionary to make the energy momentum tensor of dual field theory be well defined. These additional terms related to ϕ^4, ϕ^6 will be helpful to give to well defined boundary energy momentum tensor for the second black hole solution. The total action now becomes

$$\begin{aligned}
I_{\text{ren}} &= S_{\text{5D}} + S_{\text{GH}} + S_{\text{count}} \\
&= \frac{1}{16\pi G_5} \int_M d^5x \sqrt{-g^E} \left(R - \frac{4}{3} \partial_\mu \phi \partial^\mu \phi - V_E(\phi) - \frac{Z(\phi)}{4g_9^2} F_{\mu\nu} F^{\mu\nu} \right) \\
&\quad - \frac{1}{16\pi G_5} \int_{\partial M} d^4x \sqrt{-\gamma} \left[2K - \frac{6}{L} + \frac{8\lambda_2 \phi^2}{3L} + \frac{64\lambda_4 \phi^4}{9L^2} + \frac{512\lambda_6 \phi^6}{81L^3} \right],
\end{aligned} \tag{4.1}$$

with $\lambda_2, \lambda_4, \lambda_6$ are coefficients of count terms ϕ^2, ϕ^4, ϕ^6 introduced here. These coefficients can be fixed by canceling the divergences of boundary momentum tensor. Here K_{ij} and K are respectively the extrinsic curvature and its trace of the boundary ∂M , γ_{ij} is the induced metric on the boundary ∂M . These quantities are defined as follows

$$\gamma_{\mu\nu} = g_{\mu\nu} + n_\mu n_\nu, \quad (4.2)$$

$$K_{\mu\nu} = h_\nu^\lambda D_\lambda n_\mu, \quad (4.3)$$

$$\gamma = \det(\gamma_{\mu\nu}), \quad (4.4)$$

$$K = g^{\mu\nu} K_{\mu\nu}, \quad (4.5)$$

where $\gamma_{\mu\nu}$ denotes the induced metric, n_μ stands for the normal direction to the boundary surface ∂M as well as D_λ stands for covariant derivative.

In the asymptotical AdS space, the boundary surface locates at $z = 0$ surface, and usually one has to regularized it to a finite $z = \epsilon$ surface. So we have the normalized normal vector $n_\mu = \frac{\delta_z^\mu}{\sqrt{g_{zz}}}$.

The first term of the last line in (4.1) is Gibbons-Hawking term S_{GH} and the remain terms are related to counter terms S_{count} related to cosmological constant and dilaton field.

To regulate the theory, we restrict to the region $z \geq \epsilon$ and the surface term is evaluated at $z = \epsilon$. The induced metric is $\gamma_{ij} = \frac{\tilde{L}^2}{\epsilon^2} g_{ij}(x, \epsilon)$, where the leading term of expansion of $g_{ij}(x, \epsilon)$ with respect to ϵ is the flat metric $g_{(0)}^{ij}$. Then the one point function of stress-energy tensor of the dual CFT is given by [51][52]

$$T_{ij} = \frac{2}{\sqrt{-\det g_{(0)}}} \frac{\delta I_{\text{ren}}}{\delta g_{(0)}^{ij}} = \lim_{\epsilon \rightarrow 0} \left(\frac{L^2}{\epsilon^2} \frac{2}{\sqrt{-\gamma}} \frac{\delta I_{\text{ren}}}{\delta \gamma^{ij}} \right). \quad (4.6)$$

The finite part of boundary energy-stress tensor is from the $O(\epsilon^2)$ of the Brown-York tensor T_{ij}^{BY} on the boundary $z = \epsilon$, with

$$T_{ij}^{BY} = -\frac{1}{16\pi G_5} \left[(K_{ij} - (K + \frac{d-2}{L} + \frac{\lambda_2}{L} \phi(\epsilon)^2 + \frac{\lambda_4}{L^2} \phi(\epsilon)^4 + \frac{\lambda_6}{L^3} \phi(\epsilon)^6) \gamma_{ij}) \right], \quad (4.7)$$

In the first black solution, the coefficients of count terms can be following

$$\begin{aligned} \lambda_2 &= \frac{1}{4}, \\ \lambda_4 &= 0, \\ \lambda_6 &= 0. \end{aligned} \quad (4.8)$$

Directly evaluate (4.7) using (4.6), we get

$$T_{tt} = \frac{L^3}{16\pi G_5} \left(\frac{3}{2} f_{41} - p_1 \left(\frac{2p_1^3}{81} + \frac{2}{3} p_3 \right) \right). \quad (4.9)$$

One can see we can only introduce the ϕ^2 term to cancel the action to make the boundary energy momentum tensor be well defined. These higher powers of ϕ , such as ϕ^4, ϕ^6 terms, are not necessary to be included.

The tt component of energy tensor on the UV boundary of the second black hole solution

$$T_{tt} = \frac{L^3}{16\pi G_5} \left(\frac{3f_{42}}{2} - \frac{p_{\frac{1}{2}}^8}{5511240} - \frac{p_{\frac{1}{2}} p_{\frac{7}{2}}}{2} \right). \quad (4.10)$$

To obtain the well defined boundary energy momentum tensor, it is necessary to introduce ϕ^2, ϕ^4, ϕ^6 terms. The coefficients of these terms can be determined by canceling the divergences of boundary energy momentum tensor. In this case, one should introduce the additional term ϕ^4, ϕ^6 terms to obtain the finite boundary momentum tensor. This aspect is different from the previous case. Here we list the coefficients of related counter terms

$$\begin{aligned} \lambda_2 &= \frac{1}{8}, \\ \lambda_4 &= \frac{L}{1152}, \\ \lambda_6 &= \frac{L^2}{414720}. \end{aligned} \quad (4.11)$$

In terms of the results, one can introduce more powers of ϕ terms as a strategy to cancel the divergences of boundary energy momentum tensor for more general Einstein dilaton system. Here we just only take two groups of solutions as examples to show how to obtain the finite energy momentum tensor on the boundary.

4.2 The difference of free energy

In this subsection, we would like to study the difference of free energy between thermal gas and Euclidean black hole². In terms of total Euclidean action given in (4.1), we can obtain on-shell action for black hole as following

$$\begin{aligned} S_{5D-BH} &= 2 \int d^3x \int_0^\beta d\tau \int_0^{z_h} dz \partial_z (b_{eb}^2 b'_{eb} f_b) = 2V_3 \beta (b_{eb}^2 b'_{eb} f)|_\epsilon^{z_h} \\ S_{GH-BH} &= V_3 \beta \left(b_{eb}^3(\epsilon) f'_b(\epsilon) + 8b_{eb}^2(\epsilon) b'_{eb}(\epsilon) f_b(\epsilon) \right) \end{aligned} \quad (4.12)$$

with $b_{eb}(z) = \frac{e^{A_{eb}(z)}}{z} = \frac{e^{A_{sb}(z) - \frac{2}{3}\phi_b(z)}}{z}$, the period of Euclidean time $\beta = \frac{1}{T}$ and volume of space V_3 . Here $S_{BHcount}$ is given by (4.1) with insertion of thermal gas solution and ϵ is the regularized point. Here we also used eqs.(A.5) and (A.24) to obtain (4.12). Due to that ϕ_b satisfies the asymptotical AdS boundary condition, $S_{BHcount} = 0$. Hence it is not necessary to consider the contribution from $S_{BHcount}$.

In term of (4.12), one replace A_{eb}, f_b with A_{et}, f_t to calculate the free energy of thermal gas which is only dependent on UV behavior of conformal factor $b_{et}(z)$ in the following way

$$\begin{aligned} S_{TG}^{\text{reg}} &= S_{5D-TG} + S_{GH} + S_{TGcount}, \\ &= \frac{1}{16\pi G_5} \lim_{\tilde{\epsilon} \rightarrow 0} \tilde{\beta}(\tilde{\epsilon}) \tilde{V}_3(\tilde{\epsilon}) \left(6b_{et}^2(\tilde{\epsilon}) b'_{et}(\tilde{\epsilon}) \right) + S_{TGcount}, \end{aligned} \quad (4.13)$$

²In this subsection, all studies are based on Euclidean version of gravity solution. In this paper, we denote thermal gas solutions as Euclidean version of zero temperature solutions.

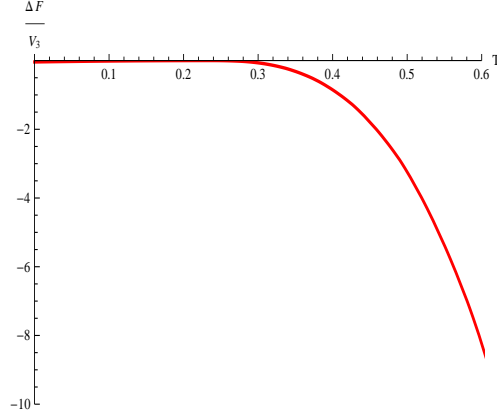


Figure 9. The difference of free energy of black hole and thermal gas in the first group solution. Here we choose the parameter $p_1 = 1.5\text{GeV}$.

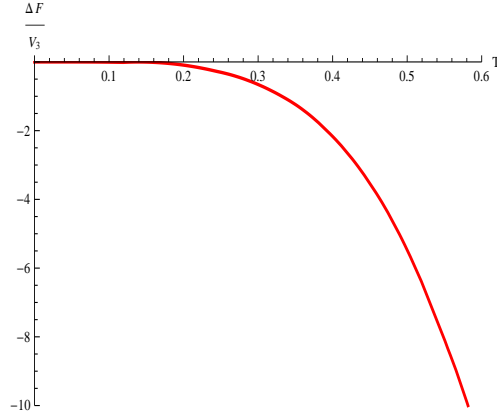


Figure 10. The difference of free energy of black hole and thermal gas in the second group. Here we choose the parameter $p_{\frac{1}{2}} = 1\text{GeV}^{\frac{1}{2}}$.

with $b_{et} = \frac{e^{A_{et}}}{z}$, the period of Euclidean time $\tilde{\beta} = \frac{1}{T}$ and volume of space \tilde{V}_3 . Where S_{TGcount} is given by (4.1) with insertion of thermal gas solution. We have checked that for thermal gas solution, the integral of the Einstein-Hilbert action extends on the region $(0, z_{IR})$, where z_{IR} is the IR cutoff and the IR contribution vanishes whenever $6b_{et}^2(z_{IR})b'_{et}(z_{IR}) \rightarrow 0$ as $z \rightarrow z_{IR}$. For these two thermal gas solutions, the IR contribution vanishes as $z \rightarrow z_{IR}$. Due to the fact that ϕ_t satisfy with the asymptotical AdS boundary condition, $S_{\text{TGcount}} = 0$. Here it is not necessary to consider the contribution from S_{TGcount} .

In order to compare the free energy between black hole and thermal gas, we should match the following conditions[55]

$$b_{et}(\tilde{\epsilon})\tilde{\beta}(\tilde{\epsilon}) = b_{eb}(\epsilon)\beta(\epsilon)\sqrt{g(\epsilon)}, \quad b_{et}(\tilde{\epsilon})^3\tilde{V}_3(\tilde{\epsilon}) = b_{eb}(\epsilon)^3V_3(\epsilon). \quad (4.14)$$

Here $\epsilon, \tilde{\epsilon}$ are different UV cutoff in black hole and thermal gas solution respectively. One should match $\phi_{th}(\tilde{\epsilon}) = \phi_b(\epsilon)$ to obtain the relationship between ϵ and $\tilde{\epsilon}$. In terms of the

relationship, one can obtain the difference of on shell action between thermal gas and black hole

$$S_{\text{BH-TG}} = -\frac{\beta V_3}{16\pi G_5} \left(\lim_{\epsilon \rightarrow 0} \left(b_{eb}^3(\epsilon) f'_b(\epsilon) + 6b_{eb}^2(\epsilon) b'_{eb}(\epsilon) f_b(\epsilon) \right) + S_{\text{BHcount}} \right) + \left(\frac{b_{eb}^4(\epsilon) \sqrt{f_b(\epsilon)}}{b_{et}^4(\tilde{\epsilon})} 6b_{et}^2(\tilde{\epsilon}) b'_{et}(\tilde{\epsilon}) + S_{\text{TGcount}} \right). \quad (4.15)$$

One can see the formula (4.15) ³ is consistent with on shell action [47] in EDM system with $U(1)$ gauge field turned off. The difference of free energy $\beta\Delta F = S_{\text{BH-TG}}$ between thermal gas and black hole are always negative as shown in Fig. 9 and 10 which correspond to the first and second group of solutions respectively. Here the ΔF denotes the difference of free energies between them. In Fig. 9 and 10, we just set parameters to show the difference of free energy between black hole and thermal gas. As we can see in Fig. 9 and 10, the black hole solutions will go back to thermal gas solution when the temperature decreases to zero. In the whole region $T \geq 0$, black holes solutions are favored in these two groups of solutions. Here one should note that these thermal gas solutions are obtained by compactifying the time direction into a circle without considering back reaction of equation of state of thermal gas. Therefore, black hole phases is more stable than thermal gas phases in these two groups of gravity solutions as shown in Fig. 9 and 10 in this level. We also would like to mention that in Fig. 9 and 10, ΔF is always negative although its absolute value is very small when T is not large enough.

5 Entanglement temperature

As applications of these solutions from AdS/CFT point of view, we consider the novel quantity called entanglement temperature in non-conformal cases [21][53][54] for our solutions. It is highly nontrivial to consider the dynamical entanglement temperature. Now we have generated two zero temperature solutions and the corresponding black hole solutions. Previous studies in above sections have shown that the black hole solutions can go back to zero temperature solutions. In this sense, that is to say black hole solutions are thermal states of zero temperature solutions in our cases. It is necessary to check whether there exists the first law of thermodynamics for EE in this system.

5.1 Variation of entanglement entropy in strip case

In this subsection, we consider the subsystem with a stripe profile which is defined by $-\frac{L_s}{2} < x_1 \equiv x < \frac{L_s}{2}$ and $-\frac{R_0}{2} < x_2, x_3 < \frac{R_0}{2}$ where R_0 , as a cutoff, is the lengthes of x_2, x_3 direction. Then the induced metric $h_{\mu\nu}$ of the bulk surface after perturbation (or thermal excitation) in the Einstein frame is

$$\frac{L^2 e^{2A_e(z)}}{z^2} \left(\frac{1}{f(z)} + x'(z)^2 \right) dz^2 + \left(\frac{L^2 e^{2A_e(z)}}{z^2} \right) dx_1^2 + \left(\frac{L^2 e^{2A_e(z)}}{z^2} \right) dx_2^2, \quad (5.1)$$

³Here we use the Euclidean action to calculate the difference of free energy. Our results is consistent with [55].

where x is a function of z , $x = x(z)$ and the prime stands for the derivative with respect to z in this subsection. We get the following volume of the submanifold which can thought as an action

$$S = \frac{L^3 R_0^2}{16\pi G_5} \int dz \frac{1}{z^3} \sqrt{\frac{e^{6A_e(z)}(1 + f(z)x'(z)^2)}{f(z)}}. \quad (5.2)$$

By minimizing the functional (5.2) to obtain the classical configuration, we get the following equation of motion

$$x''(z) + \frac{f(z)x'(z)^3(3zA'_e(z) - 3)}{z} + \frac{x'(z)(2f(z)(3zA'_e(z) - 3) + zf'(z))}{2zf(z)} = 0. \quad (5.3)$$

The solution is

$$\begin{aligned} L_s(z_0) &= 2 \int_0^{z_0} \frac{z^3}{\sqrt{(e^{6A_e(z)} - 6A_e(z_0)z_0^6 - z^6)f(z)}} dz \\ &= 2z_0 \int_0^1 \frac{t^3}{\sqrt{(e^{6A_e(z_0 t)} - 6A_e(z_0) - t^6)f(z_0 t)}} dt, \end{aligned} \quad (5.4)$$

where z_0 is the maximal value of z on the surface in the bulk, which is also called the turning point. Here the turning point is defined by $x'|_{z=z_0} = \infty$ and the boundary conditions give $x|_{z=0} = \pm L_s/2$. We only care about the case that the size L_s of subsystem satisfies $L_s \ll R_0$ which means $z_0 \ll R_0$. We have checked that $L_s(z_0)$ is monotonic function of z_0 numerically. And one can show that $z_0 \ll R_0$ is equivalent to $L_s \ll R_0$.

Under this approximation, eq. (5.4) can be expressed by following simple form.

$$L_s(z_0) = \frac{2\sqrt{\pi}\Gamma\left(\frac{2}{3}\right)z_0}{\sqrt{f_{b,th}(0)}\Gamma\left(\frac{1}{6}\right)} + O(z_0), \quad (5.5)$$

where $f(z) = f_{b,th}$ correspond to configuration of black hole and zero temperature solution respectively. We have expanded the integrand in (5.4) in power series of z_0 and performed the integration to obtain the $L_s(z_0)$ in case of $z_0 \ll R_0$.

The entanglement entropy in zero temperature solution is

$$\begin{aligned} S_{th} &= \frac{L^3 R_0^2}{8\pi G_5} \int_0^{z_0} \frac{dz}{z^3} \sqrt{\frac{z_0^6 e^{12A_{et}(z)}}{f_{th}(z)(z_0^6 e^{6f_t(z)} - z^6 e^{6A_{et}(z_0)}})} \\ &= \frac{L^3 R_0^2}{8\pi G_5 z_0^2} \int_0^1 \frac{dt}{t^3} \sqrt{\frac{z_0^6 e^{12A_{et}(z_0 t)}}{f_t(z_0 t)(z_0^6 e^{6f_t(z_0 t)} - (z_0 t)^6 e^{6A_{et}(z_0)}})} \end{aligned} \quad (5.6)$$

The entanglement entropy S_b in black hole can be obtained by replace $A_{eth}, \phi_{th}, f_{th}$ with A_{eb}, ϕ_b, f_b . Here S_{th}, S_b have not been regularized. If one is only interested in the variation of entanglement entropy, one can find that the two integrands in S_{th}, S_b have the same behavior near $z \sim 0$.

Now we introduce the counter terms for S_{th} to resolve the divergent of integrand at $t = 0$,

$$\begin{aligned}
S_{thEEcut} = & \frac{L^3 R_0^2}{8\pi G_5} \int_0^1 dt \left(\frac{e^{3A_{et}(0)}}{\sqrt{f_t(0)} t^3 z_0^2} + \frac{e^{3A_{et}(0)} (6f_t(0)A'_{et}(0) - f'_t(0))}{2f_t(0)^{3/2} t^2 z_0} \right. \\
& + \frac{e^{3A_{et}(0)} (-12f_t(0)f'_t(0)A'_{et}(0) + 36f_t(0)^2 A'_{et}(0)^2)}{8f_t(0)^{5/2} t} \\
& + \frac{e^{3A_{et}(0)} (12f_t(0)^2 A''_{et}(0) - 2f_t(0)f''_t(0) + 3f'_t(0)^2)}{8f_t(0)^{5/2} t} \Big) \\
& + \left(- \frac{e^{3A_{et}(0)} (6f_t(0)z_0 A'_{et}(0) - z_0 f'_t(0) + f_t(0))}{2f_t(0)^{3/2} z_0^2} \right) \tag{5.7}
\end{aligned}$$

Where the final term comes from compensation to deal with divergent. Combining (5.6) and (5.7) will lead to $S_{th}^{reg} = S_{th} - S_{thEEcut}$ with putting the geometrical functions $A_{et} = A_{etn}$, $f_t = f_{tn}$, $\phi_t = \phi_{tn}$ with $n = 1, 2$.⁴ In term of (5.6) and (5.7), one just only replace A_{et} , f_t with A_{eb} , f_b to obtain S_b^{reg} . Finally, the variation of entanglement entropy

$$\Delta S = S_b^{reg} - S_{th}^{reg}. \tag{5.8}$$

In the following part, we consider the black hole as low thermal excitation of zero temperature solution and calculate the difference of entanglement entropy between them approximately.

5.2 Entanglement temperature in strip case

[35] has proposed a universal relation between the variance of the energy and the entanglement entropy for a small subsystem on the boundary theory. The universal relation induce a novel concept called entanglement temperature. The $t-t$ component of the energy-stress tensor [51][52] corresponds to the energy density (4.9) and (4.10) in first and second black hole solution respectively.

For the finite stripe, the variance of entanglement entropy (5.8) in the subsystem of the first group of gravity solutions is

$$\begin{aligned}
\Delta S_{fst} = & \frac{(0.350546f_{41} - 0.409903p_1p_3)L^3 R_0^2}{8\pi G_5} z_0 \\
= & \frac{(0.350546f_{41} - 0.409903p_1p_3)L^3 R_0^2}{8\pi G_5} \frac{L_s^2 \Gamma(\frac{1}{6})^2}{\pi^2 \Gamma(\frac{2}{3})^2}. \tag{5.9}
\end{aligned}$$

Where $p_{t1} = p_{b1} = p_1$, $f_{t41} = 0$, $p_3 = 0$ and $f_{b41} = f_{41}$, $p_{b3} = p_3$.⁵ On the other hand, the increased amount of energy in the subsystem with strip configuration is given by

$$\begin{aligned}
\Delta E = & \int dx^3 \left(T_{tt}^{b1} - T_{tt}^{t1} \right), \\
= & \frac{L^3 R_0^2 L_s}{8\pi G_5} \left(\frac{3}{2} f_{41} - \frac{2}{3} p_1 p_3 \right). \tag{5.10}
\end{aligned}$$

⁴In this paper, we just use A_{ebn} , f_{bn} , ϕ_{bn} to denote the n -th black hole solutions and A_{etn} , f_{tn} , ϕ_{tn} stand for n -th zero temperature solutions.

⁵To make the notation clear, p_{t1} , f_{t41} , p_{t3} and p_{b1} , f_{b41} , p_{b3} denote the coefficients of thermal gas (or the zero temperature solution) and black hole respectively in the first group of solutions.

Where T_{tt}^{b1} and T_{tt}^{t1} stand for the tt component of boundary energy momentum tensor in black hole and zero temperature in first group solutions respectively. For the exact formula about T_{tt} , we refer to eq. (4.9). For $p_1 = 0$, the first zero temperature solution and the first black hole solution will go back to the case [35] and the variation of entanglement entropy⁶ and boundary energy momentum tensor also reproduce boundary momentum tensor given in [35].

The entanglement temperature in the first black hole is

$$\begin{aligned} \frac{1}{T_{ent}} &= \frac{\Delta S_{fst}}{\Delta E_{fst}} \\ &= \frac{(0.350546f_{41} - 0.409903p_1p_3)}{(\frac{3}{2}f_{41} - \frac{2}{3}p_1p_3)} \frac{L_s\Gamma(\frac{1}{6})^2}{\pi^2\Gamma(\frac{2}{3})^2}. \end{aligned} \quad (5.11)$$

One can find that the $T_{ent} \sim [E]$ through dimensional analysis with $[f_{41}] = [E^4]$, $[p_1] = [E^1]$, $[p_3] = [E^3]$, $[L_s] = [E^{-1}]$. Here R_0 is considered as the character length of the subsystem on the boundary. In terms of the dimensional analysis, one can see the coefficient highly depends on the geometry and shape of strip. In the first group of solutions, we fix the $p_1 = 1.5GeV$ for convenience to study the entanglement temperature without loss of generality. From our numerical study, f_{41}, p_3 are not independent and they are fixed by horizon condition $f(z_h) = 0$. In this sense, f_{41}, p_3 are functions of the position of black hole horizon z_h or black hole temperature. In our cases, we just only turn on small f_{41} or p_3 to control the temperature shown in Fig. 11. The temperature $T = \frac{f_{b1}(z)'}{4\pi}|_{z=z_h}$ increases with f_{41} and p_3 decreases simultaneously in the first black hole solution. The temperature goes from zero to small positive value which corresponds to that f_{41} increases from zero to small positive value. At the same time, the behavior of p_3 decreases from zero to negative value monotonically. In terms of (5.11), both of the nominator and denominator in (5.11) are all positive⁷ and the entanglement temperature are positive which is consistent with thermodynamical first law like proposed by [35].

For the finite stripe, the variance of entanglement entropy (5.8) in the subsystem of the second background is

$$\begin{aligned} \Delta S_{snd} &= \frac{(0.350546f_{42} - 0.23911p_{\frac{7}{2}}p_{\frac{1}{2}})L^3R_0^2}{8\pi G_5} z_0^{\frac{3}{2}} \\ &= \frac{(0.350546f_{42} - 0.23911p_{\frac{7}{2}}p_{\frac{1}{2}})L^3R_0^2}{8\pi G_5} \frac{L_s^2\Gamma(\frac{1}{6})^2}{\pi^2\Gamma(\frac{2}{3})^2}. \end{aligned} \quad (5.12)$$

Where $p_{t2} = p_{b21} = p_2$, $f_{t42} = 0$, $p_{\frac{7}{2}t} = 0$ and $f_{b42} = f_{42}$, $p_{\frac{7}{2}b} = p_{\frac{7}{2}}$ ⁸. The increased amount

⁶The variation of entanglement entropy (5.9)(5.12) is consistent with [35] up to normalization factor in $p_1 = p_{\frac{1}{2}} = 0$ cases.

⁷We have checked this statement for $p_1 \geq 0$ numerically. It is hard to prove it analytically due to the relation between f_{41} and p_3 controlled by black hole horizon at this stage.

⁸ $p_{\frac{1}{2}t}, f_{t42}, p_{\frac{7}{2}t}$ and $p_{\frac{1}{2}b}, f_{b42}, p_{\frac{7}{2}b}$ denote the coefficients of the zero temperature solution and the black hole respectively in the second group of solutions.

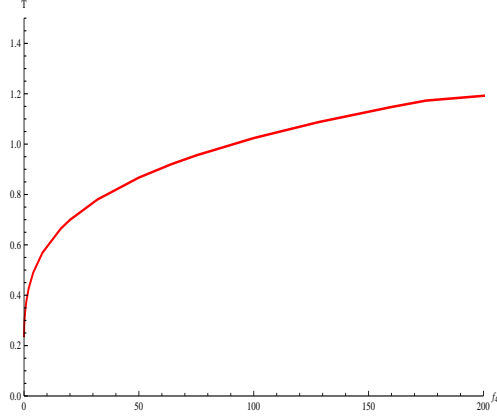


Figure 11. T v.s. f_{41} in the first solution when $p_1 = 1.5\text{GeV}$.

of energy in the subsystem with strip configuration is given by

$$\begin{aligned}\Delta E &= \int dx^3 \left(T_{tt}^{b2} - T_{tt}^{t2} \right), \\ &= \frac{L^3 R_0^2 L_s}{8\pi G_5} \left(\frac{3f_{42}}{2} - \frac{p_{\frac{1}{2}} p_{\frac{7}{2}}}{2} \right).\end{aligned}\quad (5.13)$$

Where T_{tt}^{b2} and T_{tt}^{t2} stand for the tt component of boundary energy momentum tensor in black hole and zero temperature solution in second group solutions respectively. The exact formula about T_{tt} is given in eq. (4.10). For $p_{\frac{1}{2}} = 0$, the second zero temperature solution will go back to case [35] and the variation of entanglement entropy and boundary energy momentum tensor are also consistent with boundary momentum tensor given in [35].

The entanglement temperature in the second black hole is

$$\begin{aligned}\frac{1}{T_{ent}} &= \frac{\Delta S_{snd}}{\Delta E_{snd}} \\ &= \frac{(0.350546f_{42} - 0.23911p_{\frac{7}{2}}p_{\frac{1}{2}}) L_s \Gamma(\frac{1}{6})^2}{\left(\frac{3f_{42}}{2} - \frac{p_{\frac{1}{2}} p_{\frac{7}{2}}}{2} \right) \pi^2 \Gamma(\frac{2}{3})^2}\end{aligned}\quad (5.14)$$

One can also find that the $T_{ent} \sim [E]$ through dimensional analysis with $[f_{42}] = [E^4]$, $[\mu] = [E^1]$, $[p_n] = [E^n]$, $[L_s] = [E^{-1}]$. In the second group of solutions, we fix the $p_{\frac{1}{2}} = 1\text{GeV}$ for convenience to study the entanglement temperature without losing generality. From our numerical study, $f_{42}, p_{\frac{7}{2}}$ are not independent and they are fixed by horizon condition $f_{b1}(z_h) = 0$. In this sense, $f_{42}, p_{\frac{7}{2}}$ are functions of the position of black hole horizon z_h or black hole temperature. In our cases, we turn on small f_{42} or $p_{\frac{7}{2}}$ to control the temperature shown in figures [12]. The black hole temperature $T = \frac{f_{b2}(z)'|_{z=z_h}}{4\pi}$ increases with f_{42} and $p_{\frac{7}{2}}$ decreases simultaneously in the second black hole solution. The temperature goes from zero to small positive value which corresponds to that f_{42} increases from zero to small positive value. At the same time, the behavior of $p_{\frac{7}{2}}$ decreases from zero to negative value

monotonically. In terms of (5.14), the nominator and denominator of (5.14) are all positive⁹ and the entanglement temperature are positive which is the same as previous case.

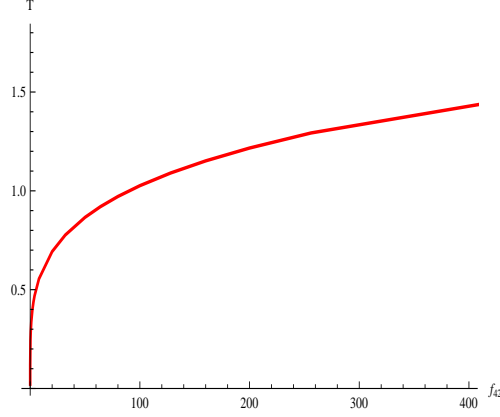


Figure 12. T v.s. f_{42} in the second solution when $p_{\frac{1}{2}} = 1\text{GeV}^{\frac{1}{2}}$.

One can see that the entanglement temperatures (5.11) (5.14) denote the first law relation of thermodynamics for EE in these two non-conformal cases from holographic perspective. One can note that entanglement temperature (5.11)(5.14) can reproduce that given in [35] with $p_1 = p_{\frac{1}{2}} = 0$. For non-conformal cases $p_1 = p_{\frac{1}{2}} \neq 0$, entanglement temperatures are also related to both UV and IR geometries which characterized by p_1 or $p_{\frac{1}{2}}$ and f_{41}, p_3 or $f_{42}, p_{\frac{7}{2}}$ respectively. In the first group of solutions, the parameter p_3 is related to condensation of the dimension 3 operator \mathcal{O}_3 ¹⁰ which holographically dual to scalar ϕ_{b1} at special temperature. The exact relation can be read out from asymptotic expansion of holographic coordinate z near UV region from (3.13) in terms of holography dictionary. In this case, the temperature is determined by the f_{41} with fixing non-vanishing source p_1 . In the second group of solutions, due to the bulk mass of ϕ_{b2} , $\frac{1}{653184} \left(653184 p_{\frac{7}{2}} - 5 p_{\frac{1}{2}}^7 \right)$ corresponds to condensation of operator $\mathcal{O}_{\frac{7}{2}}$ with dimension $\frac{7}{2}$ living on the boundary. Where the condensation is induced by the source $p_{\frac{1}{2}}$. From (3.22), one can easily read out the relation between the source and condensation of corresponding operator in the same way. Here we still have no idea about exact physical meaning of these operators partly due to that we take a bottom-up approach. One should note that there should be two ways quantize $\phi_{b1, b2}$ by imposing Dirichlet or Neumann conditions at the aAdS boundary, which are often called standard and alternative quantization respectively, and lead to two different QFTs. The analogy analysis can be done in the same way and we do not repeat here. Therefore, non-conformal entanglement temperatures do not only depend on geometric data of the subsystem but also data of gauge theory living on the boundary.

⁹We also have checked this statement for $p_{\frac{1}{2}} \geq 0$ numerically.

¹⁰In terms of holographic dictionary $\Delta_{\pm} = \frac{1}{2}(d \pm \sqrt{d^2 + 4M^2})$, $M_{\phi_{b1}}^2 = -3$ and $\langle \mathcal{O}_3 \rangle = \sqrt{\frac{8}{3}} p_3$. Where d is dimension of field theory and $M, M_{\phi_{b1}}$ are the normalized bulk mass of scalar field. At same time, $M_{\phi_{b2}}^2 = -\frac{7}{4}$ and $\langle \mathcal{O}_{\frac{7}{2}} \rangle = \sqrt{\frac{8}{3}} \frac{1}{653184} \left(653184 p_{\frac{7}{2}} - 5 p_{\frac{1}{2}}^7 \right)$.

6 Conclusion and discussion

In this paper, motivated by studying the dynamics of entanglement entropy from Einstein equation in ED system, we make use of novel technology called potential reconstruction approach to generate general gravity solutions in EDM system and we further study the entanglement temperature with Maxwell field turned off. The potential reconstruction provides an easy way to investigate novel quantities such as entanglement temperature in complicated non-conformal system from holographical point of view.

Firstly, we generate various gravity solutions within this approach and one can find that the scalar potential appeared in total action depends not only on configurations of fields but also on integral constants, such as f_{41}, f_{42} which are related to temperature. This is an effective method to obtain gravity solutions. For simplify our analysis, we fix the scalar potential to be independent of any other parameters except cosmological constant. Through some guess works, one can obtain some zero temperature solutions as we show in section 3. In order to study entanglement temperature, one should turn on thermal excitation of zero temperature solution which corresponds to the black hole solution in this paper. There is strong constrains that the black hole solution can go back to zero temperature solution continuously by tuning some temperature parameters f_{bn} . Therefore, to find black hole solution in fixed scalar potential is not an easy job here. Here we proposed a numerical way to find corresponding black hole solution to avoid the parameters dependence of dilaton potential.

Secondly, in order to study the stability of the thermal gas solution and Euclidean black hole solution, we also compute the free energy of them through introducing finite powers of ϕ terms as counter terms. In these two groups of solutions, the difference of free energy between thermal gas and black hole shows that thermal gas solution is more unstable than the corresponding black hole solution. In this sense, we consider the black hole solution as an stable thermal excitation of zero temperature solution. The entanglement entropy is a candidate for entropy in non-equilibrium physics. It is important to study the fundamental properties of entanglement entropy in order to understand non-equilibrium physics. In this paper, we have tuned some numerical parameter which is dual to black hole temperature to excite zero temperature solution. After the thermal excitation, we also study the holographic entanglement temperature and check that the first law of thermodynamics for HEE also exists in these two groups of solutions dynamically. This study lead us to understanding of non-equilibrium physics as well.

In the future, we would like to study the entanglement temperature and entanglement density in EDM system. Furthermore, it is also worth to try and check whether the first and second laws for HEE are correct in theories dual to gravity coupled with more general matter fields and/or with quantum corrections included [40]. Finally, the authors of [44][48][47][50] have used potential construction approach to generate some gravity solutions analytically. We can also make use of our numerical methods to obtain other phases. It is possible to study the properties of these phases. In appendix B, we list various asymptotical AdS_5 solutions and some of them are good places to study gauge/gravity correspondence in the bottom-up approach.

Acknowledgements

The authors are grateful to Rong-Gen Cai, Zhoujian Cao, Wu-Zhong Guo, Mei Huang, Li Li, Hong Lu, Bin Qin, Jun Tao, Yu Tian, Jian-Feng Wu, Jie Yang, Jia-Ju Zhang for useful conversations and correspondence. Further we should thank Tadashi Takayanagi for his nice suggestions and comments on this version. This work was supported in part by the National Natural Science Foundation of China a (No.10821504 (SH), No.10975168 (SH), No.11035008 (SH), No.11305235(SH), No. 11105154 (JW), and No. 11222549 (JW)), and in part by Shanghai Key Laboratory of Particle Physics and Cosmology under grant No.11DZ2230700. SH also would like appreciate the general financial support from China Postdoctoral Science Foundation No. 2012M510562. JW gratefully acknowledges the support of K. C. Wong Education Foundation and Youth Innovation Promotion Association, CAS as well.

A Appendix: Search of the Black Hole Solution Numerically

With $U(1)$ gauge field turned off in Eq.(2.2), the system will be reduced to Einstein-dilaton system as following form

$$S_{GD} = \frac{1}{16\pi G_5} \int d^5x \sqrt{-g^E} \left(R - \frac{4}{3} \partial_\mu \phi \partial^\mu \phi - V_E(\phi) \right) \quad (\text{A.1})$$

The Einstein equation and the field equation for the dilaton field are,

$$E_{MN} + \frac{1}{2} g_{MN}^E \left(\frac{4}{3} \partial_l \phi \partial^l \phi + V_E(\phi) \right) - \frac{4}{3} \partial_M \phi \partial_N \phi = 0, \quad (\text{A.2})$$

$$\frac{8}{3\sqrt{g^E}} \partial_M (\sqrt{g^E} \partial^M \phi) - \partial_\phi V_E(\phi) = 0, \quad (\text{A.3})$$

with $E_{MN} = R_{MN} - \frac{1}{2} g_{MN}^E R$.

Contracting all Lorentz indices in (A.2), we can obtain

$$-\frac{3}{2}R + \frac{5}{2} \left(\frac{4}{3} \partial_l \phi \partial^l \phi + V_E(\phi) \right) - \frac{4}{3} \partial_l \phi \partial^l \phi = 0 \quad (\text{A.4})$$

Inserting this equation to Eq.(A.1), we get the on-shell action as

$$S_{on-shell} = \int d^5x \sqrt{-g^E} \left(\frac{2}{3} V_E(\phi) \right). \quad (\text{A.5})$$

Then we would like to find the black hole solution in such ED system numerically. With taking the 4D symmetry and the asymptotically AdS condition into account, the metric ansatz would be taken as

$$dS^2 = b_e^2(z) (-f(z) dt^2 + dx_i dx^i + \frac{1}{f(z)} dz^2) \quad (\text{A.6})$$

With this ansatz, the geometric quantities can be calculated as

$$R_{tt} = \frac{2b_e'^2}{b_e^2}f^2 + \frac{5b_e'}{2b_e}ff' + \frac{b_e''}{b_e}f^2 + \frac{1}{2}ff'' \quad (\text{A.7})$$

$$R_{zz} = -\frac{4b_e''}{b_e} + \frac{4b_e'^2}{b_e^2} - \frac{5b_e'}{2b_e}\frac{f'}{f} - \frac{f''}{2f(z)} \quad (\text{A.8})$$

$$R_{ii} = -\frac{2b_e'^2}{b_e^2}f - \frac{b_e'}{b_e}f' - \frac{b_e''}{b_e}f = -\frac{\partial_z(b_e'b_e^2f)}{b_e^3} \quad (\text{A.9})$$

$$R = -\frac{8f(z)b_e''}{b_e^3} - \frac{8b_e'f'(z)}{b_e^3} - \frac{4f(z)b_e'^2}{b_e^4} - \frac{f''}{b_e^2} \quad (\text{A.10})$$

We assume that all the quantities depend on the holographic direction z only. Then the nontrivial component of Eq.(A.2) are only tt zz ii components. Together with Eq.(A.3), there're 4 non-trivial equations

$$E_{tt} + \frac{1}{2}g_{tt}(\frac{4}{3}\phi'^2g^{zz} + V_E(\phi)) = 0 \quad (\text{A.11})$$

$$E_{zz} + \frac{1}{2}g_{zz}(\frac{4}{3}\phi'^2g^{zz} + V_E(\phi)) - \frac{4}{3}\phi'^2 = 0 \quad (\text{A.12})$$

$$E_{ii} + \frac{1}{2}g_{ii}(\frac{4}{3}\phi'^2g^{zz} + V_E(\phi)) = 0 \quad (\text{A.13})$$

$$\frac{8}{3\sqrt{g}}\partial_z(\sqrt{g}g^{zz}\partial_z\phi) - \partial_\phi V_E(\phi) = 0 \quad (\text{A.14})$$

These equations can be written as,

$$\frac{2E_{tt}}{g_{tt}} + \frac{4}{3}\phi'^2g^{zz} + V_E(\phi) = 0 \quad (\text{A.15})$$

$$\frac{2E_{ii}}{g_{ii}} + \frac{4}{3}\phi'^2g^{zz} + V_E(\phi) = 0 \quad (\text{A.16})$$

$$\frac{2E_{zz}}{g_{zz}} - \frac{4}{3}\phi'^2g^{zz} + V_E(\phi) = 0 \quad (\text{A.17})$$

$$\partial_\phi V_E(\phi) = \partial_z V_E(\phi)/\phi' = \partial_z \left(-\frac{2E_{tt}}{g_{tt}} - \frac{4}{3}\phi'^2g^{zz} \right) / \phi' \quad (\text{A.18})$$

Then, we can further rearrange these equations as follows

$$V_E(\phi) = \frac{E_{zz}}{g_{zz}} + \frac{E_{tt}}{g_{tt}} = -3g^{ii}R_{ii} = -3\frac{\partial_z(b_e'b_e^2f)}{b_e^5} \quad (\text{A.19})$$

$$\frac{4}{3}\phi'^2g^{zz} = \frac{E_{zz}}{g_{zz}} - \frac{E_{tt}}{g_{tt}} = \frac{R_{zz}}{g_{zz}} - \frac{R_{tt}}{g_{tt}} = -3\frac{f}{b_e^2}\left(\frac{b_e''}{b_e} - 2\frac{b_e'^2}{b_e^2}\right) \quad (\text{A.20})$$

$$0 = \frac{E_{ii}}{g_{ii}} - \frac{E_{tt}}{g_{tt}} = \frac{R_{ii}}{g_{ii}} - \frac{R_{tt}}{g_{tt}} = -\frac{1}{2b_e^2}(f'' + 3\frac{b_e'}{b_e}f') \quad (\text{A.21})$$

So the simplified equations of motion are,

$$-\frac{b_e''}{b_e} + 2\frac{b_e'^2}{b_e^2} = \frac{4}{9}\phi'^2 \quad (\text{A.22})$$

$$f'' + 3\frac{b_e'}{b_e}f' = 0 \quad (\text{A.23})$$

$$-3\frac{\partial_z(b_e' b_e^2 f)}{b_e^5} = V_E(\phi) \quad (\text{A.24})$$

$$\frac{8}{3b_e^5}\partial_z(b_e^3 f \partial_z \phi) - \partial_\phi V_E(\phi) = 0 \quad (\text{A.25})$$

One should note that these four equations are not independent. (A.22)(A.23) are 2nd order differential equations. One of (A.24) and (A.25) is constrain equation. In order to set our numerical strategy, we choose (A.22)(A.23)(A.25) to find numerical solution and use (A.24) as consistent condition to check the numerical solution. This can be understood from that

$$\partial_z V_E(\phi) = \phi' \partial_\phi V_E(\phi) = \frac{8\phi'}{3\sqrt{g}} \partial_z(\sqrt{g} g^{zz} \phi') \quad (\text{A.26})$$

$$= \frac{1}{\sqrt{g}} \left(2\partial_z(\sqrt{g} g^{zz}) \left(\frac{4}{3}\phi'^2\right) + \sqrt{g} g^{zz} \partial_z \left(\frac{4}{3}\phi'^2\right) \right) \quad (\text{A.27})$$

$$= -\frac{3}{b_e^5} \left(2\partial_z(b_e^3 f) \left(\frac{b_e''}{b_e} - 2\frac{b_e'^2}{b_e^2}\right) + b_e^3 f \partial_z \left(\frac{b_e''}{b_e} - 2\frac{b_e'^2}{b_e^2}\right) \right) \quad (\text{A.28})$$

$$= -3\partial_z \left(\frac{\partial_z(b_e^2 b_e' f)}{b_e^5} \right) + \frac{3b_e'(3b_e' f' + b_e f'')}{b_e^4}. \quad (\text{A.29})$$

So from Eq.(A.22)(A.23)(A.25), we can get

$$\partial_z \left(3\frac{\partial_z(b_e' b_e^2 f)}{b_e^5} + V_E(\phi) \right) = 0 \quad (\text{A.30})$$

and if the initial condition guarantees that Eq.(A.24) is satisfied at a certain z , Eq. (A.24) would be satisfied for all z . So the four equations are not independent. We would only use Eq.(A.22)(A.23)(A.25) in the numeric process, and guarantee that Eq.(A.24) using the initial condition. Finally, there are total five integral constants which should be fixed. These five constants will be fixed later.

A.1 The first numerical black hole solution

We take $V_{E1}(\phi) = -\frac{12}{L^2} - \frac{9 \sinh^2(\frac{2\phi}{3})}{L^2}$, the first analytic solution can be generated by potential reconstruction approach

$$\phi_{t1}(z) = p_1 z \quad (\text{A.31})$$

$$A_{et1}(z) = \log \left(\frac{\frac{2}{3} p_1 z}{\sinh(\frac{2}{3} p_1 z)} \right) \quad (\text{A.32})$$

$$f_{t1}(z) = 1. \quad (\text{A.33})$$

Then we try to find a asymptotic AdS black hole solution numerically. In order to show this algorithm to obtain numerical solution, we assume the expansion of $\phi(z)$ as

$$\phi_{b1}(z) = p_{\Delta} z^{\Delta} + p_{4-\Delta} z^{4-\Delta} + \dots \quad (\text{A.34})$$

The power order of z can be determine $\Delta = 1$ (or equivalently $\Delta = 3$) from the mass term in $V(\phi)$. We use series expansion of unknown functions as follows

$$\phi_{b1}(z) = p_1 z + p_3 z^3 + \Sigma_n p_n z^n \quad (\text{A.35})$$

$$A_{eb1}(z) = \Sigma_n a_n z^n \quad (\text{A.36})$$

$$f_{b1}(z) = 1 + \Sigma_n f_n z^n \quad (\text{A.37})$$

One should note these power orders of z for each unknown function should be consistent with Einstein equations. The other parameters p_n, a_n, f_n ¹¹ can be determined by equations of motion. Here $f_{b1}(0)$ is set to be one to satisfy the asymptotical AdS boundary.

In terms of the equation of motion, the series expansion can be determined in terms of coefficients p_3, f_{41} which can be considered as the integral constants of these differential equations. In some sense, these coefficients p_1, p_3, f_{41} stand for IR boundary conditions. The results are as following, with the even powers of $\phi_{b1}(z)$ and odd powers of $A_{eb1}(z), f_{b1}(z)$ being always vanishing,

$$\phi_{b1}(z) = p_1 z + p_3 z^3 + \frac{z^5 (405 f_{41} p_1 + 612 p_1^2 p_3)}{3240} + \dots \quad (\text{A.38})$$

$$A_{eb1}(z) = -\frac{2 p_1^2 z^2}{27} + z^4 \left(\frac{4 p_1^4}{3645} - \frac{2 p_1 p_3}{15} \right) + \dots \quad (\text{A.39})$$

$$f_{b1}(z) = 1 - f_{41} z^4 - \frac{4}{27} f_{41} p_1^2 z^6 + \dots \quad (\text{A.40})$$

Without loss of generality, we would fix $p_1 = \frac{3}{2} \text{GeV}$ as a setting of the energy scale in all the calculations. In order to get a black hole solution, we would try to get a solution with a pole in $f_{b1}(z)$. $f_{b1}(z)$ should decrease monotonously from the initial value $f_{b1}(z=0) = 1$ to $f_{b1}(z_h) = 0$. Where z_h denotes the event horizon of the black hole. Re-writing eq.(A.25) in terms of A_{eb1} , it becomes

$$\phi_{b1}'' - \left(\frac{3}{z} - 3 A_{e1}' \right) \phi_{b1}' - \frac{-8 f_{b1}' z^2 \phi_{b1}' + 3 e^{2 A_{eb1}} L^2 \partial_{\phi_{b1}} V_{Et1}(\phi)}{8 z^2 f_{b1}} = 0, \quad (\text{A.41})$$

and due to $f_{b1}(z_h) = 0$, z_h would be a singular point of the equation. To resolve this issue, the solution should satisfy that $-8 f_{b1}' z^2 \phi_{b1}' + 3 e^{2 A_{eb1}} L^2 \partial_{\phi_{b1}} V_{Et1}(\phi) = 0$ at $z = z_h$ and this condition would impose a constrain on the acceptable value of the two integral constants p_3, f_{41} with p_1 fixed, i.e. if we take a certain f_{41} , only a certain value of $p_3 = p_3(f_{41})$ can create a black hole solution. Varying f_{41} would be related to varying the temperature of the black hole.

¹¹One should note that $f_4 = f_{41}$ in this case.

To show how the above procedure works explicitly, we take $f_{41} = 0.75$ as an example. For further convenience, we define a $\text{Test}(z)$ function

$$\text{Test}(z) \equiv -8f'_{b1}z^2\phi'_{b1} + 3e^{2A_{et1}}L^2\partial_{\phi_{b1}}V_{Et1}(\phi). \quad (\text{A.42})$$

The shooting method can find the exact z_h , such that $f_{b1}(z_h) = \text{Test}(z_h) = 0$. Here we will fix $p_1 = 3/2, f_{41} = 0.75$ to show how to find z_h in Fig. 13(a)(b).

We choose $p_3 = -0.1$, and insert this three integral constants into Eqs. (A.35)(A.36)(A.37). Then we fix the $p_1 = \frac{3}{2}$ to find the exact relation between p_3 and f_{41} . The relation can be fixed by IR boundary condition $f_b(z_h) = 0$ and $\text{Test}(z_h) = 0$ simultaneously. Here we can use shoot method to find the exact z_h and then p_3, f_{41} can be determined finally. In Fig. 13, we just tune p_3 with f_{41} fixed to try to find the exact z_h numerically. Recall that z_h satisfies $f_b(z_h) = 0$ and $\text{Test}(z_h) = 0$. That is to say p_3 and f_{41} are not independent and there are relations among them and z_h . This is very important in studying entanglement temperature. Fig. 13 shows that how to find z_h and p_3 with f_{41} fixed. In Fig. 13(a), one can vary p_3 with f_{41} fixed and find that the blue solid line and the blue dashed line cross the same point in x axis which means horizon has been found. In Fig. 13(b), we just show $\text{Test}(z)$ explicitly to confirm that there is one z_h such that $\text{Test}(z_h) = f_{b1}(z_h) = 0$ for each p_3 .

To closed this section, we should summarize the algorithm. Firstly, one should figure out the series expansion of unknown function $\phi_{b1}(z), A_{Et1}(z), f_{b1}(z)$ with asymptotical AdS boundary condition. Here asymptotical AdS boundary condition can fix 2 integral constants. Secondly, one can find three integral constants determined by IR boundary conditions and $\text{Test}(z)$. Finally, finding the horizon position and one of integral constants with shooting method will fix the final two integral constants. After these three steps, all integral constants can be fixed numerically and one can put them into the Einstein equations to produce numerical black hole solution in this system.

A.2 The second numerical black hole solution

Following the arithmetic given in subsection A.1, we would like to find the second numerical black hole with potential $V_{Et2} = -\frac{27}{4L^2} - \frac{21 \cosh\left(\frac{2\sqrt{2}\phi}{3}\right)}{4L^2}$. Here one should note that the powers order of z is not integer anymore, since they are constrained by Einstein equation. Here we do not repeat numerical analysis procedure as in the previous section.¹² We just choose various parameters to obtain the corresponding black hole solution in the same way. Here we follow the same steps to find the exact z_h shown in Fig. 14. In Fig. 14, one can vary $p_{\frac{7}{2}}$ with fixing f_{42} and find that the blue solid line and the blue dashed line cross the same point in x axis which means z_h has been found. Here the blue solid line and the blue dashed line stands for $\text{Test}(z)$ and $f_{b2}(z)$ respectively. Where $\text{Test}(z)$ defined by (A.42) with replacing subscript index $b1$ with $b2$. In Fig. 14(b), we just show $\text{Test}(z)$ explicitly to confirm that there is one z_h such that $\text{Test}(z_h) = f_{b2}(z_h) = 0$ for each $p_{\frac{7}{2}}$. Once z_h is fixed with given $p_{\frac{1}{2}}$, the black hole solution can be obtained numerically.

¹²If reader would like to repeat the above analysis mentioned in (A.1), you can only replace all the subscript index $b1$ of these functions with $b2$.

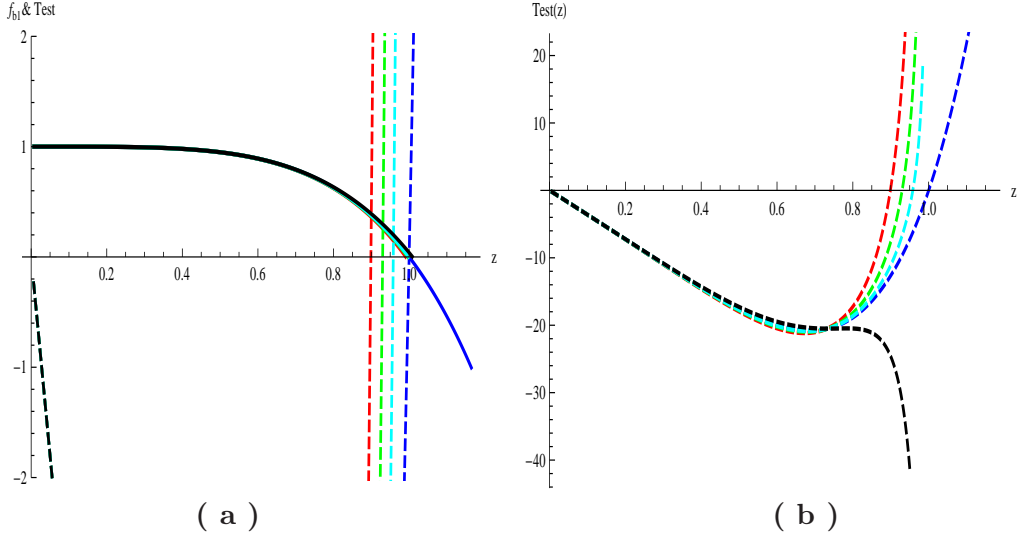


Figure 13. The behavior of $f_{b1}(z)$ and $\text{Test}(z)$ when p_3 varies and $p_1 = 1.5, f_{41} = 0.75$. The solid lines and dashed lines stands for $f_{b1}(z)$ and $\text{Test}(z)$ respectively. And the Red, Green, Cyan, Blue, Black line stand for $p_3 = -0.1, -0.15, -0.175, -0.18697, -0.3$ respectively.

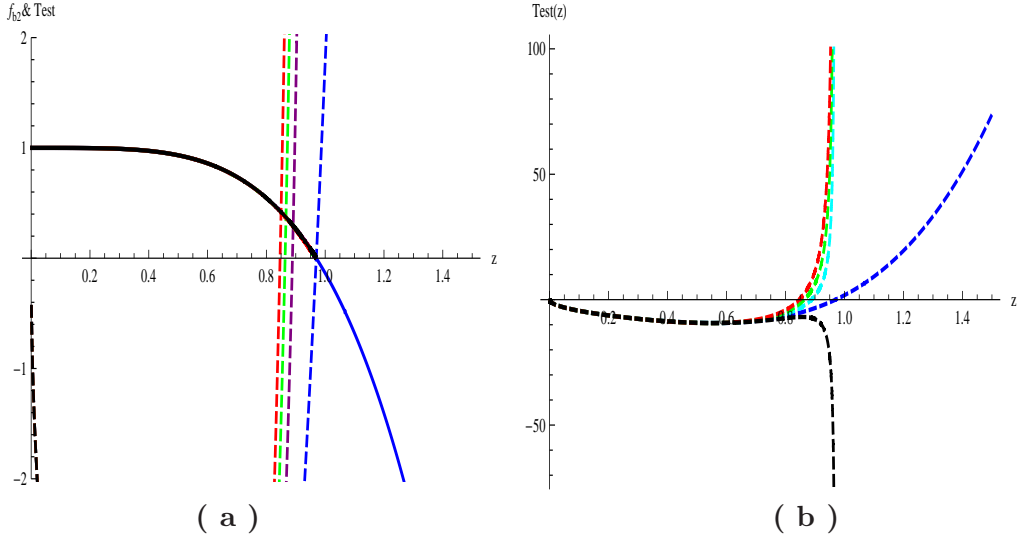


Figure 14. The behavior of $f_{b2}(z)$ and $\text{Test}(z)$ when $p_{\frac{7}{2}}$ varies and $p_{\frac{1}{2}} = 1, f_{42} = 1$. The solid lines and dashed lines stands for $f_{b2}(z)$ and $\text{Test}(z)$ respectively. The Red, Green, Cyan, Blue, Black line stand for $p_{\frac{7}{2}} = -0.01, -0.03, -0.05, -0.0706084, -0.09$ respectively.

B Other Analytic Solutions

In this subsection, we would like to list other analytic solutions generated by potential reconstruction approach in this paper. At this stage, we have not studied related properties of these solutions. It is interesting to study these solutions with asymptotical AdS boundary condition from holographical point of view in the future. Here we just only list other 4

solutions of ED system (A.1) with following ansatz

$$ds_E^2 = \frac{L^2 e^{2A_{en}}}{z^2} \left(-f_n(z) dt^2 + \frac{dz^2}{f_n(z)} + dx^i dx^i \right). \quad (\text{B.1})$$

Where n denotes different solutions.

The 3rd solution is

$$A_{e3}(z) = \log(1 - \mu_3 z) \quad (\text{B.2})$$

$$\phi_3(z) = -3\sqrt{2} \arctan(\sqrt{\mu_3 z}) \quad (\text{B.3})$$

$$f_3(z) = 1 + f_{43} \left(-\frac{3}{2} + (1 - \mu_3 z) + \frac{3}{1 - \mu_3 z} - \frac{1}{2(1 - \mu_3 z)} + 3 \log(1 - \mu_3 z) \right) \quad (\text{B.4})$$

$$V_{E3}(\phi_3) = -\frac{1}{32L^2} 3 \cosh^4\left(\frac{\phi_3}{3\sqrt{2}}\right) \quad (\text{B.5})$$

$$(f_{43} \cosh(\sqrt{2}\phi_3) + 168f_{43} \log\left(\text{sech}^2\left(\frac{\phi_3}{3\sqrt{2}}\right)\right)) \quad (\text{B.6})$$

$$+ \cosh\left(\frac{2\sqrt{2}\phi_3}{3}\right) \left(24f_{43} \log\left(\text{sech}^2\left(\frac{\phi_3}{3\sqrt{2}}\right)\right) + 42f_{43} + 8 \right) \quad (\text{B.7})$$

$$+ \cosh\left(\frac{\sqrt{2}\phi_3}{3}\right) \left(192f_{43} \log\left(\text{sech}^2\left(\frac{\phi_3}{3\sqrt{2}}\right)\right) + 15f_{43} + 64 \right) - 58f_{43} + 56) \quad (\text{B.8})$$

Where μ_3, f_{43} are integral constants and L stands for asymptotical AdS radius.

The 4th solution can be expressed

$$A_{e4}(z) = -\log\left(1 + \frac{\mu_4^2 z^2}{3(1 + \mu_4 z)}\right) \quad (\text{B.9})$$

$$\phi_4(z) = \frac{3\sqrt{2}}{2} \log(1 + \mu_4 z) \quad (\text{B.10})$$

$$f_4(z) = 1 - f_{44} \frac{14 - 81(1 + \mu_4 z)^2 + 84(1 + \mu_4 z)^3 - 21(1 + \mu_4 z)^6 + 4(1 + \mu_4 z)^9}{756(1 + \mu_4 z)^2} \quad (\text{B.11})$$

$$V_{E4}(\phi_4) = -\frac{14e^{\frac{2\sqrt{2}\phi_4}{3}}}{3L^2} - \frac{20e^{-\frac{1}{3}(\sqrt{2}\phi_4)}}{3L^2} - \frac{2e^{-\frac{1}{3}(4\sqrt{2}\phi_4)}}{3L^2} + \quad (\text{B.12})$$

$$\frac{f_{44}}{L^2} \left(-\frac{5e^{-\frac{1}{3}(\sqrt{2}\phi_4)}}{7} + \frac{2e^{-\sqrt{2}\phi_4}}{9} - \frac{e^{-\frac{1}{3}(4\sqrt{2}\phi_4)}}{14} + \frac{5e^{\sqrt{2}\phi_4}}{21} - \frac{e^{2\sqrt{2}\phi_4}}{126} - \frac{e^{\frac{2\sqrt{2}\phi_4}{3}}}{2} + \frac{5}{6} \right), \quad (\text{B.13})$$

where μ_4, f_{44} are integral constants and L stands for asymptotical AdS radius.

The 5th solution is

$$A_{e5}(z) = -\log\left(\frac{3(-1 + (1 + \mu_5 z)^{5/3})}{5\mu_5 z(1 + \mu_5 z)^{1/3}}\right) \quad (\text{B.14})$$

$$\phi_5(z) = \log(1 + \mu_5 z) \quad (\text{B.15})$$

$$f_5(z) = 1 - f_{45}\left(\frac{9}{5}(1 + \mu_5 z)^{5/3} - \frac{9}{10}(1 + \mu_5 z)^{10/3} + \frac{1}{5}(1 + \mu_5 z)^5 - \log(1 + \mu_5 z) - \frac{11}{10}\right) \quad (\text{B.16})$$

$$V_{E5}(\phi_5) = -\frac{3e^{-\frac{8\phi_5}{3}}\left(40e^{\frac{5\phi_5}{3}} + 60e^{\frac{10\phi_5}{3}}\right)}{25L^2} - \frac{3f_{45}e^{-\frac{8\phi_5}{3}}\left(12e^{\frac{10\phi_5}{3}}(5\phi_5 - 3) + e^{\frac{20\phi_5}{3}} - 12e^{5\phi_5} + e^{\frac{5\phi_5}{3}}(40\phi_5 + 44) + 3\right)}{25L^2} \quad (\text{B.17})$$

Where μ_5, f_{45} are integral constants and L stands for asymptotical AdS radius.

The 6th solution is

$$A_{e6}(z) = -\log(1 + \mu_6^\alpha z^\alpha) \quad (\text{B.18})$$

$$\phi_6(z) = 3\sqrt{\frac{1 + \alpha}{\alpha}} \arcsin(\sqrt{\mu_6^\alpha z^\alpha}) \quad (\text{B.19})$$

$$f_6(z) = 1 - f_{46}\mu_6^4 z^4 \left(1 + \frac{12\mu_6^\alpha z^\alpha}{4 + \alpha} + \frac{6\mu_6^{2\alpha} z^{2\alpha}}{2 + \alpha} + \frac{4\mu_6^{3\alpha} z^{3\alpha}}{4 + 3\alpha}\right) \quad (\text{B.20})$$

$$\begin{aligned} V_{E6}(\phi_6) = & \frac{3(-256(3\alpha^3 + 22\alpha^2 + 48\alpha + 32))}{64(\alpha + 2)(\alpha + 4)(3\alpha + 4)L^2} \\ & + \frac{3(-32(3\alpha^4 + 25\alpha^3 + 70\alpha^2 + 80\alpha + 32))}{64(\alpha + 2)(\alpha + 4)(3\alpha + 4)L^2} \\ & + \frac{\sinh^2\left(\frac{\alpha\phi_6}{3\sqrt{\alpha(\alpha+1)}}\right)\left((3\alpha + 4)\cosh\left(\frac{2\alpha\phi_6}{3\sqrt{\alpha(\alpha+1)}}\right) - 5\alpha + 12\right)}{64(\alpha + 2)(\alpha + 4)(3\alpha + 4)L^2} \\ & + \frac{3\alpha^2(-120\alpha^3 - 134\alpha^2 - 114\alpha - 40)f_{46}\sinh^{\frac{8}{\alpha}+2}\left(\frac{\alpha\phi_6}{3\sqrt{\alpha(\alpha+1)}}\right)}{64(\alpha + 2)(\alpha + 4)(3\alpha + 4)L^2} \\ & + \frac{3\alpha^2 f_{46}\sinh^{\frac{8}{\alpha}+2}\left(\frac{\alpha\phi_6}{3\sqrt{\alpha(\alpha+1)}}\right)\left(3(24\alpha^3 - 35\alpha^2 - 49\alpha - 20)\cosh\left(\frac{2\alpha\phi_6}{3\sqrt{\alpha(\alpha+1)}}\right)\right)}{64(\alpha + 2)(\alpha + 4)(3\alpha + 4)L^2} \\ & + \frac{3\alpha^2 f_{46}\sinh^{\frac{8}{\alpha}+2}\left(\frac{\alpha\phi_6}{3\sqrt{\alpha(\alpha+1)}}\right)\left(6(5\alpha^2 - 5\alpha - 4)\cosh\left(\frac{4\alpha\phi_6}{3\sqrt{\alpha(\alpha+1)}}\right) - 4\cosh\left(\frac{2\alpha\phi_6}{\sqrt{\alpha(\alpha+1)}}\right)\right)}{64(\alpha + 2)(\alpha + 4)(3\alpha + 4)L^2} \\ & + \frac{3\alpha^2 f_{46}\sinh^{\frac{8}{\alpha}+2}\left(\frac{\alpha\phi_6}{3\sqrt{\alpha(\alpha+1)}}\right)\left(\alpha^2\cosh\left(\frac{2\alpha\phi_6}{\sqrt{\alpha(\alpha+1)}}\right) + 3\alpha\cosh\left(\frac{2\alpha\phi_6}{\sqrt{\alpha(\alpha+1)}}\right)\right)}{64(\alpha + 2)(\alpha + 4)(3\alpha + 4)L^2}, \end{aligned} \quad (\text{B.21})$$

Where μ_6, f_{46} are integral constants and L stands for asymptotical AdS radius. In this case, one can deform this solution by turning the parameter α which is useful to build up some asymptotical AdS background.

To close this subsection, we would like to add the following comments. One can use potential reconstruction approach to generate various gravity background in conformal ansatz and domain wall ansatz. One should note from the solutions given above that the geometric parameters contribute to dilaton potential $V_{E1,E2,E3,E4,E5,E6}$. Changing these parameters in the potential V_{En} with $n = 1, \dots, 6$ means that the theory is changed. In other words, different values of the parameters f_{4n}, μ_n in V_{En} correspond to different gravity theories. In some gravity solutions [44][49] reconstructed by this method, it seems inevitable that these different theories can be connected by the same form of action with different values of parameters in V_{En} . The different values of parameters corresponds to different configuration of bulk field and different potential, therefore, these theory are not equivalent to each other any more. Once one constructs gravity background, for the stability of the system, one should confirm the potential $V_{E1}, V_{E2}, V_{E3}, V_{E4}, V_{E5}, V_{E6}$ and $A_{e1,e2,e3,e4,e5,e6}(z), f_{1,2,3,4,5,6}(z), \phi_{1,2,3,4,5,6}(z)$ should satisfy the constrains from other perspectives, e.g., Breitenlohner-Freedman bound of scalar field near AdS boundary [56][57], that the total action is finite, well-defined boundary conditions of the system and so on. Generally speaking, the method is efficient and effective and using the approach needs ones to do something more to make the solution self-consistently. In order to avoid arbitrary dilaton potential generated by potential reconstruction, we arrange a systematic method to obtain zero temperature solution and the corresponding numerical black hole solution with the same dilation potential in ED system. By following the logic present in this paper, one can produce nontrivial thermal gas solutions and obtain the black hole solutions numerically. This approach is not the one from first principle (i. e. top-down) but an effective and efficient way which shed light on study of gauge/gravity duality.

References

- [1] J. M. Maldacena, “The large N limit of superconformal field theories and supergravity,” Adv. Theor. Math. Phys. **2**, 231 (1998) [Int. J. Theor. Phys. **38**, 1113 (1999)] [arXiv:hep-th/9711200].
- [2] S. S. Gubser, I. R. Klebanov and A. M. Polyakov, “Gauge theory correlators from non-critical string theory,” Phys. Lett. B **428**, 105 (1998) [arXiv:hep-th/9802109].
- [3] E. Witten, “Anti-de Sitter space and holography,” Adv. Theor. Math. Phys. **2**, 253 (1998) [arXiv:hep-th/9802150].
- [4] O. Aharony, S. S. Gubser, J. M. Maldacena, H. Ooguri and Y. Oz, “Large N field theories, string theory and gravity,” Phys. Rept. **323**, 183 (2000) [arXiv:hep-th/9905111].
- [5] S. Ryu and T. Takayanagi, “Holographic derivation of entanglement entropy from AdS/CFT,” Phys. Rev. Lett. **96**, 181602 (2006) [hep-th/0603001].
- [6] A. Lewkowycz and J. Maldacena, “Generalized gravitational entropy,” arXiv:1304.4926 [hep-th].
- [7] H. Casini, M. Huerta and R. C. Myers, “Towards a derivation of holographic entanglement entropy,” JHEP **1105**, 036 (2011) [arXiv:1102.0440 [hep-th]].
- [8] M. Headrick, “Entanglement Renyi entropies in holographic theories,” Phys. Rev. D **82**, 126010 (2010) [arXiv:1006.0047 [hep-th]].

- [9] T. Hartman, “Entanglement Entropy at Large Central Charge,” arXiv:1303.6955 [hep-th].
- [10] T. Faulkner, “The Entanglement Renyi Entropies of Disjoint Intervals in AdS/CFT,” arXiv:1303.7221 [hep-th].
- [11] T. Nishioka, S. Ryu and T. Takayanagi, ‘Holographic Entanglement Entropy: An Overview,” J. Phys. A **42**, 504008 (2009) [arXiv:0905.0932 [hep-th]].
- [12] T. Takayanagi, “Entanglement Entropy from a Holographic Viewpoint,” Class. Quant. Grav. **29**, 153001 (2012) [arXiv:1204.2450 [gr-qc]].
- [13] T. Albash and C. V. Johnson, “Holographic Entanglement Entropy and Renormalization Group Flow,” JHEP **1202**, 095 (2012) [arXiv:1110.1074 [hep-th]].
- [14] R. C. Myers and A. Singh, “Comments on Holographic Entanglement Entropy and RG Flows,” arXiv:1202.2068 [hep-th].
- [15] J. de Boer, M. Kulaxizi and A. Parnachev, “Holographic Entanglement Entropy in Lovelock Gravities,” JHEP **1107**, 109 (2011) [arXiv:1101.5781 [hep-th]].
- [16] L. -Y. Hung, R. C. Myers and M. Smolkin, “On Holographic Entanglement Entropy and Higher Curvature Gravity,” JHEP **1104**, 025 (2011) [arXiv:1101.5813 [hep-th]].
- [17] B. Chen and J. -j. Zhang, “Note on generalized gravitational entropy in Lovelock gravity,” arXiv:1305.6767 [hep-th].
- [18] A. Bhattacharyya, A. Kaviraj and A. Sinha, “Entanglement entropy in higher derivative holography,” arXiv:1305.6694 [hep-th].
- [19] T. Nishioka and T. Takayanagi, “AdS Bubbles, Entropy and Closed String Tachyons,” JHEP **0701**, 090 (2007) [hep-th/0611035].
- [20] J. -R. Sun, “Note on Chern-Simons Term Correction to Holographic Entanglement Entropy,” JHEP **0905**, 061 (2009) [arXiv:0810.0967 [hep-th]].
- [21] I. R. Klebanov, D. Kutasov and A. Murugan, “Entanglement as a probe of confinement,” Nucl. Phys. B **796**, 274 (2008) [arXiv:0709.2140 [hep-th]].
- [22] A. Pakman and A. Parnachev, “Topological Entanglement Entropy and Holography,” JHEP **0807**, 097 (2008) [arXiv:0805.1891 [hep-th]].
- [23] N. Ogawa and T. Takayanagi, “Higher Derivative Corrections to Holographic Entanglement Entropy for AdS Solitons,” JHEP **1110**, 147 (2011) [arXiv:1107.4363 [hep-th]].
- [24] R. -G. Cai, S. He, L. Li and Y. -L. Zhang, “Holographic Entanglement Entropy in Insulator/Superconductor Transition,” JHEP **1207**, 088 (2012) [arXiv:1203.6620 [hep-th]].
- [25] R. -G. Cai, S. He, L. Li and Y. -L. Zhang, “Holographic Entanglement Entropy on P-wave Superconductor Phase Transition,” JHEP **1207**, 027 (2012) [arXiv:1204.5962 [hep-th]].
- [26] R. -G. Cai, S. He, L. Li and L. -F. Li, “Entanglement Entropy and Wilson Loop in Stückelberg Holographic Insulator/Superconductor Model,” JHEP **1210**, 107 (2012) [arXiv:1209.1019 [hep-th]].
- [27] M. Nozaki, T. Numasawa and T. Takayanagi, “Holographic Local Quenches and Entanglement Density,” arXiv:1302.5703 [hep-th].
- [28] T. Hartman and J. Maldacena, “Time Evolution of Entanglement Entropy from Black Hole Interiors,” arXiv:1303.1080 [hep-th].
- [29] M. Nozaki, T. Numasawa, A. Prudenziati and T. Takayanagi, “Dynamics of Entanglement

Entropy from Einstein Equation,” arXiv:1304.7100 [hep-th].

- [30] M. B. Hastings, “An area law for one-dimensional quantum systems”, J. Stat. Mech. (2007) P08024[quant-ph/0705.2024]
- [31] M. Srednicki, “Entropy and area,” Phys. Rev. Lett. **71**, 666 (1993) [hep-th/9303048].
- [32] Francisco Castilho Alcaraz, Miguel Ibanez Berganza, German Sierra, “Entanglement of low-energy excitations in Conformal Field Theory,” Phys.Rev.Lett.106:201601,2011[arXiv:1101.2881[cond-mat]].
- [33] L. Masanes, “An Area law for the entropy of low-energy states,” Phys. Rev. A **80**, 052104 (2009) [arXiv:0907.4672 [quant-ph]].
- [34] D. Allahbakhshi, M. Alishahiha and A. Naseh, “Entanglement Thermodynamics,” arXiv:1305.2728 [hep-th].
- [35] J. Bhattacharya, M. Nozaki, T. Takayanagi and T. Ugajin, “Thermodynamical Property of Entanglement Entropy for Excited States,” Phys. Rev. Lett. 110, **091602** (2013) [arXiv:1212.1164 [hep-th]].
- [36] R. C. Myers and A. Sinha, “Seeing a c-theorem with holography,” Phys. Rev. D **82**, 046006 (2010) [arXiv:1006.1263 [hep-th]].
- [37] W. -Z. Guo, S. He and J. Tao, “Note on Entanglement Temperature for Low Thermal Excited States in Higher Derivative Gravity,” arXiv:1305.2682 [hep-th].
- [38] D. V. Fursaev, “Proof of the holographic formula for entanglement entropy,” JHEP **0609**, 018 (2006) [hep-th/0606184].
- [39] T. Barrella, X. Dong, S. A. Hartnoll and V. L. Martin, “Holographic entanglement beyond classical gravity,” arXiv:1306.4682 [hep-th].
- [40] T. Faulkner, A. Lewkowycz and J. Maldacena, “Quantum corrections to holographic entanglement entropy,” arXiv:1307.2892 [hep-th].
- [41] S. S. Gubser and A. Nellore, “Mimicking the QCD equation of state with a dual black hole,” Phys. Rev. D **78**, 086007 (2008); S. S. Gubser, A. Nellore, S. S. Pufu and F. D. Rocha, “Thermodynamics and bulk viscosity of approximate black hole duals to finite temperature quantum chromodynamics,” Phys. Rev. Lett. **101**, 131601 (2008); S. S. Gubser, S. S. Pufu and F. D. Rocha, “Bulk viscosity of strongly coupled plasmas with holographic duals,” JHEP **0808**, 085 (2008).
- [42] U. Gursoy, E. Kiritsis, L. Mazzanti and F. Nitti, “Deconfinement and Gluon Plasma Dynamics in Improved Holographic QCD,” Phys. Rev. Lett. **101**, 181601 (2008); U. Gursoy, E. Kiritsis, G. Michalogiorgakis and F. Nitti, “Thermal Transport and Drag Force in Improved Holographic QCD,” JHEP **0912**, 056 (2009).
- [43] K. Farakos, A. P. Kouretsis, P. Pasipoularides, “Anti de Sitter 5D black hole solutions with a self-interacting bulk scalar field: A Potential reconstruction approach,” Phys. Rev. **D80**, 064020 (2009). [arXiv:0905.1345 [hep-th]].
- [44] D. Li, S. He, M. Huang and Q. S. Yan, “Thermodynamics of deformed AdS₅ model with a positive/negative quadratic correction in graviton-dilaton system,” JHEP **1109**, 041 (2011) [arXiv:1103.5389 [hep-th]].
- [45] N. Ohta, T. Torii, “Black Holes in the Dilatonic Einstein-Gauss-Bonnet Theory in Various Dimensions IV: Topological Black Holes with and without Cosmological Term,” Prog. Theor.

- Phys. **122**, 1477-1500 (2009). [arXiv:0908.3918 [hep-th]].
- [46] T. Kolyvaris, G. Koutsoumbas, E. Papantonopoulos, G. Siopsis, “A New Class of Exact Hairy Black Hole Solutions,” Gen. Rel. Grav. **43**, 163-180 (2011). [arXiv:0911.1711 [hep-th]].
 - [47] R. -G. Cai, S. He and D. Li, “A hQCD model and its phase diagram in Einstein-Maxwell-Dilaton system,” JHEP **1203**, 033 (2012) [arXiv:1201.0820 [hep-th]].
 - [48] S. He, Y. -P. Hu and J. -H. Zhang, “Hydrodynamics of a 5D Einstein-dilaton black hole solution and the corresponding BPS state,” JHEP **1112**, 078 (2011) [arXiv:1111.1374 [hep-th]].
 - [49] S. He, M. Huang, Q. -S. Yan, “Logarithmic correction in the deformed AdS_5 model to produce the heavy quark potential and QCD beta function,” Phys. Rev. **D83**, 045034 (2011). [arXiv:1004.1880 [hep-ph]].
 - [50] R. -G. Cai, S. Chakraborty, S. He and L. Li, “Some aspects of QGP phase in a hQCD model,” JHEP **1302**, 068 (2013) [arXiv:1209.4512 [hep-th]].
 - [51] K. Skenderis, “Lecture notes on holographic renormalization,” Class. Quant. Grav. **19**, 5849 (2002) [hep-th/0209067].
 - [52] S. de Haro, S. N. Solodukhin and K. Skenderis, “Holographic reconstruction of space-time and renormalization in the AdS / CFT correspondence,” Commun. Math. Phys. **217**, 595 (2001) [hep-th/0002230].
 - [53] S. Ryu and T. Takayanagi, “Aspects of Holographic Entanglement Entropy,” JHEP **0608**, 045 (2006) [hep-th/0605073].
 - [54] K. Narayan, “Non-conformal brane plane waves and entanglement entropy,” arXiv:1304.6697 [hep-th].
 - [55] U. Gursoy, E. Kiritsis, L. Mazzanti and F. Nitti, “Holography and Thermodynamics of 5D Dilaton-gravity,” JHEP **0905**, 033 (2009) [arXiv:0812.0792 [hep-th]].
 - [56] P. Breitenlohner and D. Z. Freedman, “Positive Energy in anti-De Sitter Backgrounds and Gauged Extended Supergravity,” Phys. Lett. B **115**, 197 (1982).
 - [57] P. Breitenlohner and D. Z. Freedman, “Stability in Gauged Extended Supergravity,” Annals Phys. **144**, 249 (1982).